



Candida albicans Isolates 529L and CHN1 Exhibit Stable Colonization of the Murine Gastrointestinal Tract

Liam D. McDonough,^{a,b} Animesh A. Mishra,^c Nicholas Tosini,^{d,e} Pallavi Kakade,^a Swathi Penumutchu,^a Shen-Huan Liang,^a Corrine Maufrais,^f Bing Zhai,^{d,e} Ying Taur,^{d,g}  Peter Belenky,^a  Richard J. Bennett,^a  Tobias M. Hohl,^{d,e,g}  Andrew Y. Koh,^{h,i}  Iuliana V. Ene^{a,f}

^aDepartment of Molecular Microbiology and Immunology, Brown University, Providence, Rhode Island, USA

^bDepartment of Microbial Pathogenesis, Yale School of Medicine, New Haven, Connecticut, USA

^cDepartment of Microbiology, University of Texas Southwestern Medical Center, Dallas, Texas, USA

^dInfectious Disease Service, Department of Medicine, Memorial Sloan Kettering Cancer Center, New York, New York, USA

^eImmunology Program, Sloan Kettering Institute, Memorial Sloan Kettering Cancer Center, New York, New York, USA

^fDepartment of Mycology, Institut Pasteur, Paris, France

^gDepartment of Medicine, Weill Cornell Medical College, New York, New York, USA

^hDepartment of Pediatrics, University of Texas Southwestern Medical Center, Dallas, Texas, USA

ⁱHarold C. Simmons Cancer Center, University of Texas Southwestern Medical Center, Dallas, Texas, USA

Liam D. McDonough, Animesh A. Mishra, and Nicholas Tosini made equal contributions. The three co-first authors are listed alphabetically.

ABSTRACT *Candida albicans* is a pathobiont that colonizes multiple niches in the body including the gastrointestinal (GI) tract but is also responsible for both mucosal and systemic infections. Despite its prevalence as a human commensal, the murine GI tract is generally refractory to colonization with the *C. albicans* reference isolate SC5314. Here, we identify two *C. albicans* isolates, 529L and CHN1, that stably colonize the murine GI tract in three different animal facilities under conditions where SC5314 is lost from this niche. Analysis of the bacterial microbiota did not show notable differences among mice colonized with the three *C. albicans* strains. We compared the genotypes and phenotypes of these three strains and identified thousands of single nucleotide polymorphisms (SNPs) and multiple phenotypic differences, including their ability to grow and filament in response to nutritional cues. Despite striking filamentation differences under laboratory conditions, however, analysis of cell morphology in the GI tract revealed that the three isolates exhibited similar filamentation properties in this *in vivo* niche. Notably, we found that SC5314 is more sensitive to the antimicrobial peptide CRAMP, and the use of CRAMP-deficient mice modestly increased the ability of SC5314 to colonize the GI tract relative to CHN1 and 529L. These studies provide new insights into how strain-specific differences impact *C. albicans* traits in the host and advance CHN1 and 529L as relevant strains to study *C. albicans* pathobiology in its natural host niche.

IMPORTANCE Understanding how fungi colonize the GI tract is increasingly recognized as highly relevant to human health. The animal models used to study *Candida albicans* commensalism commonly rely on altering the host microbiome (via antibiotic treatment or defined diets) to establish successful GI colonization by the *C. albicans* reference isolate SC5314. Here, we characterize two *C. albicans* isolates that can colonize the murine GI tract without antibiotic treatment and can therefore be used as tools for studying fungal commensalism. Importantly, experiments were replicated in three different animal facilities and utilized three different mouse strains. Differential colonization between fungal isolates was not associated with alterations in the bacterial microbiome but rather with distinct responses to CRAMP, a host antimicrobial peptide. This work emphasizes the importance of *C. albicans* intraspecies variation as well as host antimicrobial defense mechanisms in defining the outcome of commensal interactions.

Citation McDonough LD, Mishra AA, Tosini N, Kakade P, Penumutchu S, Liang S-H, Maufrais C, Zhai B, Taur Y, Belenky P, Bennett RJ, Hohl TM, Koh AY, Ene IV. 2021. *Candida albicans* isolates 529L and CHN1 exhibit stable colonization of the murine gastrointestinal tract. *mBio* 12: e02878-21. <https://doi.org/10.1128/mBio.02878-21>.

Editor Judith Berman, Tel Aviv University

Copyright © 2021 McDonough et al. This is an open-access article distributed under the terms of the [Creative Commons Attribution 4.0 International license](https://creativecommons.org/licenses/by/4.0/).

Address correspondence to Richard J. Bennett, richard_bennett@brown.edu, Tobias M. Hohl, hohl@mskcc.org, Andrew Y. Koh, andrew.koh@utsouthwestern.edu, or Iuliana V. Ene, iuliana.ene@pasteur.fr.

This article is a direct contribution from Richard J. Bennett, a Fellow of the American Academy of Microbiology, who arranged for and secured reviews by Deborah Hogan, Dartmouth College, and Don Shepherd, McGill University.

Received 29 September 2021

Accepted 6 October 2021

Published 2 November 2021

KEYWORDS fungal biology, gastrointestinal colonization, microbiome, strain diversity

The fungal component of the human microbiota, the mycobiota, is increasingly recognized as playing key roles in host homeostasis (1–7). *Candida albicans*, a pathobiont that is found in over 70% of individuals, is a prominent member of the gastrointestinal (GI) mycobiota (8, 9). This species is present in multiple niches of the human body and can cause a variety of opportunistic mucosal and systemic infections. Disseminated infections can arise when *Candida* cells in the GI tract translocate into the bloodstream (10, 11), as has been observed in murine models of mucositis and neutropenia (12) and in patients undergoing allogeneic hematopoietic cell transplants (13). *C. albicans*, as well as other *Candida* species, is also linked to intestinal disease, with *C. albicans* consistently found at high levels in cohorts of Crohn's disease and ulcerative colitis patients (14). The loss of host signaling pathways involved in fungal recognition, such as those involving Dectin-1 or Dectin-3, may exacerbate colitis due to increased *Candida* levels in the gut (15, 16).

The impact of the GI mycobiota is not limited to gut mucosal tissues but can also modulate systemic responses distal to this organ. For example, *C. albicans* cells in the GI tract can drive the induction of systemic Th17 responses in both mice and humans (1, 4). These systemic responses are a double-edged sword as they can provide protection against systemic infections by fungi or other microbial pathogens but can cause increased airway inflammation in response to antigens in the lung (1, 4). Understanding of GI colonization by *C. albicans* and related fungal species therefore has far-reaching consequences for understanding immune homeostasis at both intestinal sites and sites distal to the gut.

Given their central role in host homeostasis, it is notable that most laboratory mice are not readily colonized with *C. albicans* or other fungi (17, 18). The importance of commensal fungi to the biology of laboratory mice was highlighted in a recent study in which lab mice were rewilded by release and subsequent recapture from an outdoor facility (17). Notably, rewilded mice showed enhanced differentiation of memory T cells and increased levels of circulating granulocytes, and these changes were associated with increased fungal colonization of the GI tract (17). Inoculation of lab mice either with fungi from rewilded mice or with *C. albicans* was sufficient to enhance immune responses, further establishing that the gut mycobiota can play broad roles in educating host immunity.

Relatively little is known about the fungal and host mechanisms that regulate GI colonization by species such as *C. albicans*. Most studies have relied on antibiotic supplementation to allow the standard "laboratory" strain of *C. albicans*, SC5314, to stably colonize the GI tract of mice (12, 19, 20). Several other *Candida* strains are also unable to colonize the murine GI tract without the use of antibiotics, including *C. albicans* strains WO-1, Can098, 3153A, ATCC 18804, and OH-1; *Candida glabrata* ATCC 15126; a *Candida parapsilosis* clinical isolate; and *Candida tropicalis* ATCC 66029 (21–24).

Antibiotic treatment against bacterial taxa can enable fungal colonization as specific bacterial commensals induce the transcription factor HIF-1 α in enterocytes which in turn leads to production of CRAMP, an antimicrobial peptide related to the human cathelicidin LL-37 (21). LL-37 has been shown to exhibit both antibacterial and antifungal activity (25) and can inhibit *Candida* adhesion and affect cell wall integrity by interacting with cell wall components, including the exoglucanase Xog1 (26–28). CRAMP kills *C. albicans* cells *in vitro* (29) and inhibits GI colonization, as shown by increased *C. albicans* colonization in mice lacking CRAMP (21). Conversely, on the fungal side, loss of filamentation has been linked to enhanced GI colonization by *C. albicans* cells in both antibiotic-treated and germ-free mice (30–33). Several transcriptional regulators of the *C. albicans* mating circuit have also been shown to impact fungal fitness levels in this niche (32, 34–36).

While SC5314 represents the standard isolate of *C. albicans* used by many in the field, several studies have established that *C. albicans* isolates display a wide range of phenotypic properties both *in vitro* and in models of infection (37–41). Intraspecies variation can therefore have a major impact on *C. albicans* strain behavior and determine the outcome of host-fungal interactions. Understanding interstrain differences is critical for determining the

breadth of properties displayed by a species and could lead to new insights into mechanisms of fungal adaptation, niche specificity, and pathogenesis (34, 42–45).

Here, we compared the abilities of different *C. albicans* strains to colonize the murine GI tract without antibiotic treatment. We identified two isolates, 529L and CHN1, that stably colonize the GI tract under conditions where SC5314 is consistently lost from this niche. Similar findings were obtained when using three different widely used mouse lines in three different animal facilities, highlighting the robustness of this finding. 529L and CHN1 also outcompeted SC5314 in direct competition experiments in the murine intestine, establishing that these strains exhibit an increased relative fitness for this niche. Analysis of the phenotypic properties of SC5314, CHN1, and 529L revealed stark differences in filamentation and metabolism among these strains *in vitro*. However, filamentation differences were not evident in the murine gut, highlighting how *in vivo* phenotypes can differ from those observed *in vitro*. Instead, we show that CHN1 and 529L were more resistant to killing by the CRAMP peptide relative to SC5314 and link these differences to GI colonization fitness using mice lacking CRAMP. Together, these studies highlight how differences between *C. albicans* isolates can dictate differences in gut colonization and establish CHN1 and 529L as powerful tools for the study of this fungus in its commensal niche.

RESULTS

***C. albicans* strains 529L and CHN1 can stably colonize the murine GI tract without antibiotics.** We compared the abilities of three *C. albicans* human isolates to each colonize the GI tract of three different strains of mice in the absence of antibiotic supplementation. The isolates tested were SC5314, the standard “laboratory” isolate originally obtained from a bloodstream infection (46); 529L, isolated from the oral cavity (47); and CHN1, isolated from the lung (48). These strains were selected following testing of several clinical isolates for their ability to colonize the GI tract of C3H/HeN mice. Each strain was orally gavaged to BALB/c (Charles River Laboratories), C57BL/6J (Jackson Laboratories), and C3H/HeN (Envigo) mice fed a standard chow diet in animal facilities in Texas (TX), New York (NY), and Rhode Island (RI). These mouse lines have been extensively used by the *Candida* community for studies of fungal infection and colonization (49–52). GI colonization levels were monitored by plating mouse fecal pellets every 2 to 7 days.

SC5314 did not stably colonize the GI tract of any of the mice tested. For example, levels of colony-forming units (CFU) decreased 1 to 2 logs in the first 7 to 14 days of infection in both C3H/HeN (TX) and C57BL/6J (RI) mice and fell below detection levels at later time points (Fig. 1A to D). In contrast, 529L and CHN1 more stably colonized the GI tract in each of the mouse strain backgrounds, particularly in C57BL/6J (RI, NY) and C3H/HeN (TX) mice, being maintained for 28 to 48 days postinoculation (Fig. 1A to D). For C57BL/6J (RI, NY) mice, colonization differences between isolates were readily apparent in the 1st week postgavage, and in the RI facility these differences increased out to 28 days of colonization (Fig. 1A and B). Most C57BL/6J mice cleared SC5314 cells whereas CHN1 and 529L were present at $>10^3$ CFU/g feces in both the NY and RI facilities at the end of the experiment (Fig. 1A and B and see Fig. S1A in the supplemental material). In BALB/c (RI) mice, 529L and CHN1 had higher levels of colonization than SC5314 during the first 5 days, although significance was not observed at later time points (Fig. 1C). Finally, in C3H/HeN (TX) mice, both 529L and CHN1 were present at higher levels than SC5314 throughout the time course with SC5314 cells no longer recovered from the fecal pellets of any mice by day 21 (Fig. 1D and Fig. S1A).

At the end of the experiment, colonization levels were also examined by recovery of CFU from GI organs in C57BL/6J and BALB/c mice. Analysis revealed relatively high levels of 529L and CHN1 present in C57BL/6J (RI) organs (average of 10^4 to 10^5 CFU/g), while SC5314 was typically not recovered from any GI organs (Fig. S1B). For BALB/c (RI) mice, we could not identify significant differences in organ colonization levels between the three isolates at day 28, reflecting the fact that each isolate showed reduced colonization at these time points in this mouse background (no detectable CFU except for one mouse in each group with 10^3 to 10^5 CFU/g [Fig. S1B]).

Having established that 529L and CHN1 showed increased fitness relative to SC5314 in monocolonization experiments, we tested whether these strains showed fitness differences

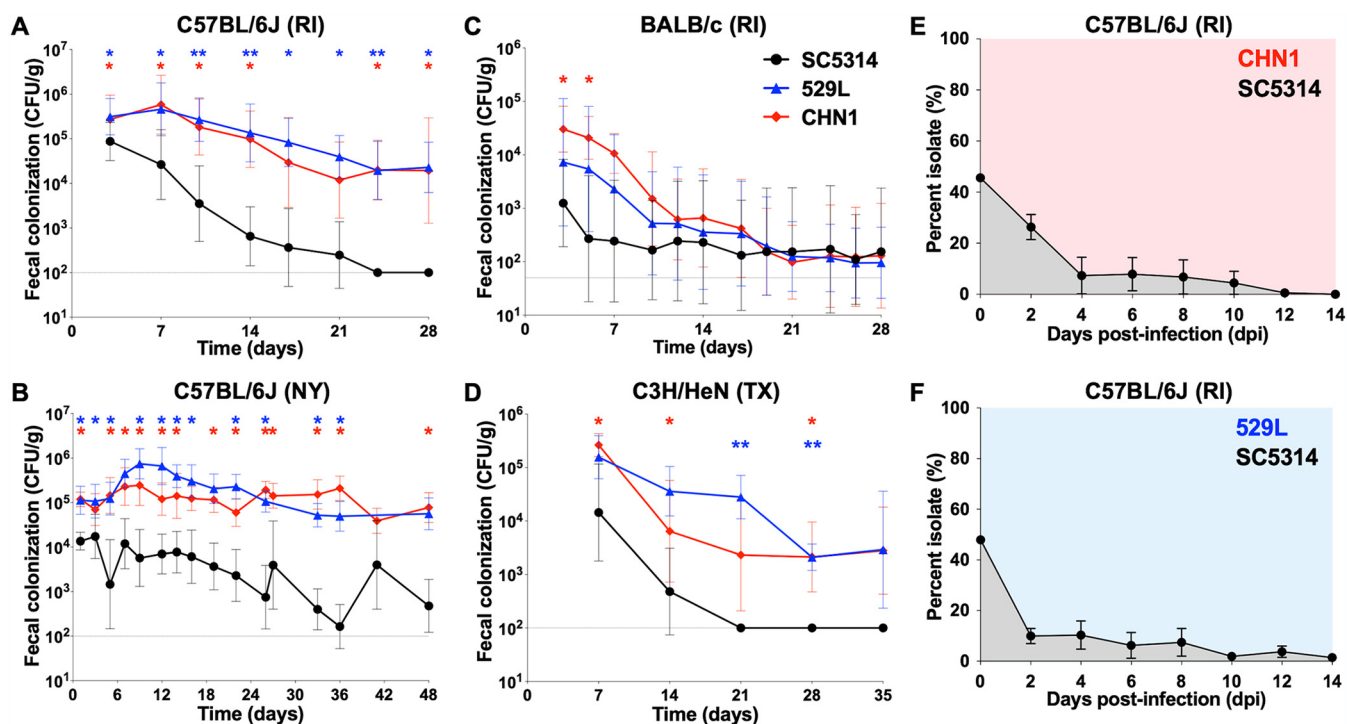


FIG 1 (A to D) *C. albicans* isolates 529L and CHN1 can stably colonize the gastrointestinal tract of C57BL/6J (A [RI, $n = 8$ mice] and B [NY, $n = 10$ to 18 mice]), BALB/c (C [RI, $n = 8$ mice]), and C3H/HeN (D [TX, $n = 8$ mice]) mice without antibiotic treatment. Panels show geometric means with 95% confidence intervals (CI) of fecal colonization levels (CFU/g) over time. Asterisks reflect comparisons between isolates at individual time points using Mann-Whitney tests: *, $P < 0.05$; **, $P < 0.01$. Horizontal lines indicate the minimum CFU detection level for each experiment (50 or 100 CFU/g fecal pellet). (E and F) Direct competitions between SC5314 and 529L (E) or CHN1 (F) in the GI tract of C57BL/6J mice (RI). Isolates were coinoculated in a 1:1 ratio, and their proportions were determined using nourseothricin selection upon recovery from fecal pellets. Panels show means \pm standard errors of the means (SEM) from 4 single-housed mice.

in direct competition experiments. To distinguish the strains in a direct competition, SC5314 was transformed with a nourseothricin resistance gene (*SAT1*) targeted to the *NEUT5L* on chromosome (Chr) 5, which is a neutral locus for integration of ectopic constructs (53). To verify that the presence of *SAT1* at this site does not alter the fitness of isolates during gut colonization, we performed competitions between SC5314 and two independently transformed SC5314 isolates containing *SAT1*. A 1:1 mix of *SAT1*-marked and unmarked SC5314 was introduced into the GI tract, and relative strain abundance was determined by calculating the proportion of nourseothricin-resistant colonies recovered from fecal pellets over 14 days. Experiments revealed no significant advantage between the two versions of SC5314, indicating that the presence of *SAT1* did not affect *C. albicans* fitness in the GI tract (Fig. S1C).

Next, a 1:1 mix of SC5314 (*SAT1* marked) and 529L or CHN1 was introduced into the GI tract, and the relative proportions of each strain were determined from fecal pellets of C57BL/6J (RI) mice. By day 4 postgavage, both 529L and CHN1 began to dominate the colonizing population, with SC5314 cells representing less than 10% of CFU in fecal pellets (Fig. 1E and F). By day 14, CHN1 and 529L accounted for 100% and 98.5% of the cells recovered from the feces, respectively, and similar proportions of isolates were observed across the different GI organs (stomach, small intestine, colon, and cecum [Fig. S2A]). We also note that similar fungal burdens were recovered from either single colonization or competition experiments, indicating that the presence of a second isolate did not significantly impact the colonization capacity of any one isolate (C57BL/6J mice [RI] [Fig. S2B]). These results indicate that both CHN1 and 529L display increased competitive fitness relative to SC5314 throughout the GI tract.

To extend these findings, we performed similar competition experiments using *SAT1*-marked/unmarked versions of each isolate in different combinations in the C57BL/6J (NY) background. Experiments mirrored the RI facility findings in that both CHN1 and

529L showed increased competitive fitness relative to SC5314 (Fig. S2C and D). Thus, 20- to 100-fold-fewer SC5314 colonies than CHN1/529L colonies were recovered from competition assays (Fig. S2F). Monocolonization with CHN1 or 529L generally resulted in higher fungal burdens than competition assays that included these strains (Fig. S2F and G). Experiments also showed that CHN1 exhibited a consistent fitness advantage over 529L in a head-to-head test (Fig. S2E).

We note, however, that large fluctuations were observed in the overall proportions of each isolate in these competitions. When competing CHN1 and SC5314, differences between strains were apparent approximately 24 days postgavage, when CHN1 became dominant in fecal pellets (Fig. S2C). For 529L versus SC5314 competitions, 529L represented ~80% of the fungal population after 3 days or after 22 days depending on which strain carried the *SAT1* gene (Fig. S2D). Similarly, the fitness advantage of CHN1 relative to 529L was evident much earlier in one competition than in the other (Fig. S2E), illustrating variability in the dynamics of gut colonization. Despite this variation, these findings establish that CHN1 and 529L consistently show increased fitness in the murine GI tract compared to SC5314.

C. albicans isolates do not significantly affect the composition of the gut bacterial microbiome. Commensal bacterial gut microbiota (particularly the phylum *Bacteroidetes* and family *Lachnospiraceae*) are important for murine resistance to *C. albicans* colonization (21), an association that was recently corroborated in adult hematopoietic cell transplant recipients (13). To assess the impact of colonization with different *C. albicans* isolates on the bacterial microbiota, the 16S rRNA hypervariable region was sequenced from fecal pellets from both BALB/c and C57BL/6J mice colonized with these isolates, with the work performed in mice housed in two different animal facilities (RI and NY). We found that colonization with SC5314, 529L, or CHN1 strains did not result in any significant differences in microbiome composition at phylum or family levels in either animal facility (Fig. 2A to C). Colonization also did not significantly affect the alpha diversity of the bacterial microbiome as measured by the Shannon diversity index or cause significant changes in beta diversity, with samples displaying no significant clustering on the principal-coordinate analysis (PCoA) projection of Bray-Curtis distances for both BALB/c (Fig. S3A) and C57BL/6J (Fig. S3B and C) mice in the two facilities (RI, NY). These experiments establish that *C. albicans* colonization with these different isolates has a minimal impact on the composition of the bacterial microbiota under the conditions evaluated in this study.

SC5314, 529L, and CHN1 show distinct metabolic and filamentation properties *in vitro*. To investigate the mechanism by which 529L and CHN1 exhibit increased GI fitness relative to SC5314, we compared the phenotypes of the three isolates in a series of *in vitro* assays. First, colony filamentation was examined on YPD, SCD, Spider, and Lee's + glucose media (Fig. 3A). Cells were plated on these media, incubated at 37°C for 4 days, and assessed for filamentation. No visible differences were noted between the three strains when grown on YPD; however, 529L displayed markedly reduced colony filamentation on SCD, Spider, and Lee's + glucose media relative to both SC5314 and CHN1. Next, cell morphology was examined under various liquid filamentation-inducing conditions after 4 h of growth at 37°C. Consistent with colony phenotypes, 529L did not efficiently filament under these conditions and only formed rare hyphae or pseudohyphae in medium supplemented with 10% fetal calf serum (Fig. 3B). In contrast, SC5314 and CHN1 displayed a strong filamentation response across all media tested.

To further characterize phenotypic differences between these strains, we utilized phenotype microarrays (PM; Biolog) containing a set of 190 different carbon sources. The three isolates were seeded on PM plates and incubated with shaking at 37°C for 24 h, both aerobically and anaerobically. Growth was evaluated by taking biomass (optical density at 600 nm [OD₆₀₀]) readings, and individual wells were assessed for filamentation using a semi-quantitative score of 1 to 5 (Table S3). A score of 1 indicates 0 to 20% hyphae observed, while a score of 5 indicates that 80 to 100% of the population formed hyphae. Under aerobic conditions, the three isolates displayed different growth capacities across carbon sources, with SC5314 being able to reach a higher biomass (mean OD₆₀₀ across wells = 0.45 ± 0.3 standard deviation [SD]) than both 529L (0.30 ± 0.17) and CHN1 (0.42 ± 0.25) (Fig. 3C, *P* < 0.01 for both isolates relative to SC5314, *df* = 191, two-way analysis of variance [ANOVA]). Although

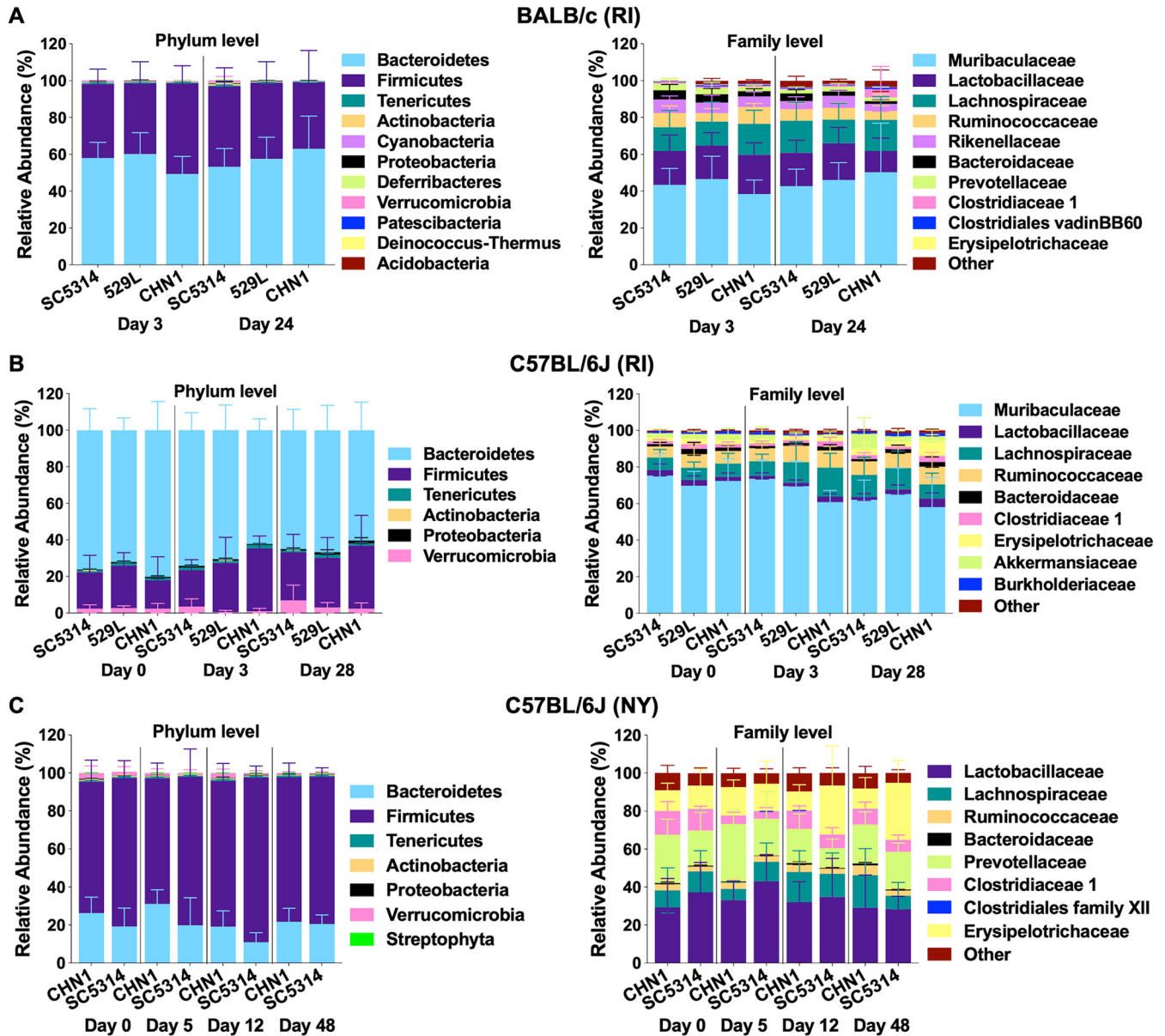


FIG 2 Microbiome composition of BALB/c (A [RI]) and C57BL/6J (B [RI] or C [NY]) mice colonized with *C. albicans* isolates SC5314, CHN1, or 529L. Plots show microbiome relative abundances at the phylum and family levels for mice from Fig. 1. Day 0 time points indicate the microbiome composition prior to *Candida* gavage.

smaller, differences in growth were also apparent when the isolates were incubated anaerobically (Fig. 3C, $P < 0.0001$ for both 529L and CHN1 relative to SC5314). Analysis of filamentation under aerobic conditions revealed that 529L again displayed a severe filamentation defect across the surveyed carbon sources (average filamentation score 1.2 ± 0.5), while CHN1 displayed an intermediate filamentation capacity (1.8 ± 0.6) compared to SC5314 (2.8 ± 0.8) [Fig. 3C], $P < 0.0001$ for both comparisons). Similar results were observed when comparing filamentation capacities of the three isolates under low-oxygen conditions (Fig. 3C, $P < 0.0001$ comparing SC5314 to 529L or CHN1).

Increased *C. albicans* GI colonization has been previously associated with decreased levels of short-chain or medium-chain fatty acids (54, 55). In addition, the presence of short-chain carboxylic acids has been shown to reduce *C. albicans* filamentation by modulating external pH, and this effect could promote gut colonization (56–59). We therefore assessed the impact of carboxylic acids (acetic, butyric, lactic, capric, succinic, propionic, and citric acid) on the ability of the three strains to grow and form filaments.

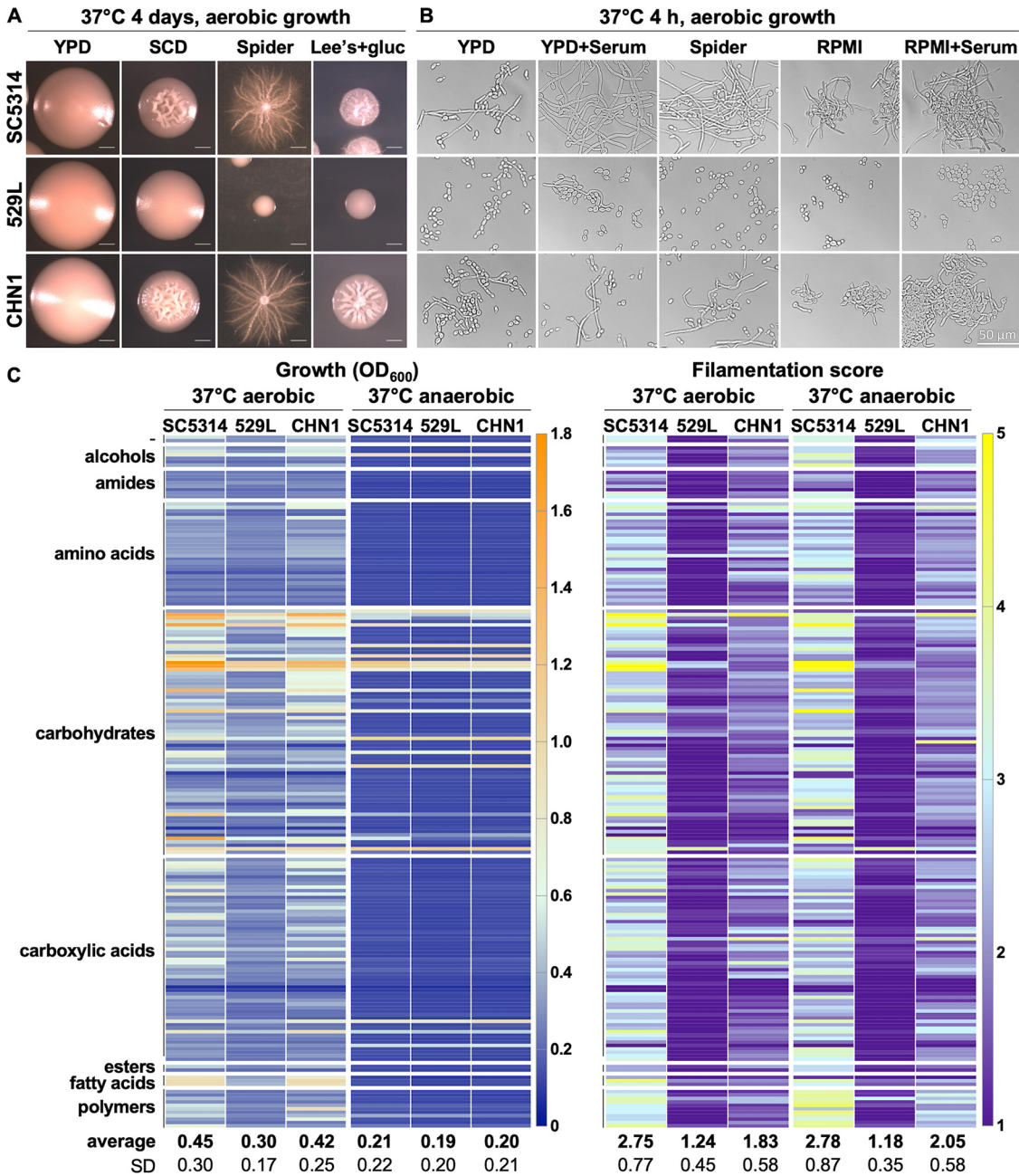


FIG 3 *In vitro* growth and filamentation of isolates SC5314, CHN1, and 529L in different laboratory media and nutritional conditions. (A and B) Colony (A) and cell (B) morphology of isolates grown at 37°C under aerobic conditions in different laboratory media. Scale bars, 1 mm (A) and 50 μm (B). (C) Growth and filamentation of isolates SC5314, CHN1, and 529L on Biolog carbon source plates (PM01-02) under aerobic and anaerobic conditions. Carbon sources are grouped according to their biochemical group. After 24 h of growth at 37°C, each well was scored for filamentation on a 1-to-5 scale (1 and 5 represent conditions where 0 to 20% and 80 to 100% of cells showed visible filamentation, respectively). Values under each column indicate means ± SD from two biological replicates for each condition.

Aerobic growth on short-chain carboxylic acids revealed that CHN1 and 529L showed reduced filamentation relative to SC5314, with a larger defect observed for 529L ($P < 0.01$ for both isolates relative to SC5314, $df = 9$, two-way ANOVA), which also displayed reduced growth ($P < 0.05$, Fig. S4A). Differences in filamentation were also observed for 529L under anaerobic conditions ($P < 0.01$, relative to SC5314), whereas the three isolates showed similar growth on this subset of carboxylic acids (Fig. S4A).

While it is possible that reduced filamentation could simply be the result of reduced growth, a correlation analysis between growth and filamentation levels across all

carbon sources tested revealed that this was not the case (Fig. S4B). This was most apparent when the three isolates were grown under anaerobic conditions—a simple linear regression resulted in a goodness of fit with R^2 of 0 to 0.14, indicating the absence of a correlation between growth and filamentation across these conditions (Fig. S4B). Overall, these results indicate that both 529L and CHN1 have reduced *in vitro* growth and filamentation capacities relative to SC5314, with these differences being more pronounced for 529L.

SC5314, 529L, and CHN1 show extensive genetic differences. Previous reports have associated the presence of *C. albicans* aneuploid chromosomes with increased fitness for particular host niches, including trisomy of Chr 6, which was repeatedly selected for during oral infection (60), and trisomy of Chr 7, which favored colonization of the mouse GI tract (61). Thus, we examined the whole-genome sequences of the three isolates to identify genetic changes that could contribute to differential colonization of this niche. 529L and SC5314 have been previously sequenced (38, 62); therefore, only CHN1 was *de novo* sequenced for this study. All three isolates were compared to the SC5314 reference genome (assembly 22) and comparative genomic analyses were performed between CHN1/529L and the SC5314 version examined here. Phylogenetic analysis revealed that CHN1 and 529L isolates belong to the relatively rare clades A and 16, respectively, whereas SC5314 belongs to clade 1 (38, 42). This analysis also reveals that 529L and CHN1 are more closely related to each other than they are to SC5314 (42).

We found that all three isolates were euploid across all chromosomes (Fig. S5A), eliminating aneuploidy of specific chromosomes as a potential explanation for differences in GI fitness. However, the isolates displayed differences in heterozygosity patterns across their genome, with large homozygous regions (0.1 to 0.87 Mbp) present on multiple chromosomes (Fig. S5B and C). Certain homozygous regions were shared in the 529L and CHN1 whole-genome sequences, with telomeric regions of Chr 7R and Chr RR displaying minimal heterozygosity (Fig. S5B and C). Variant calling comparing 529L and CHN1 with SC5314 revealed 112,057 and 86,513 variants, respectively (Fig. S5D and detailed in Table S4). Approximately 48% of all variants were found in coding regions, with ~90% of the total variants represented by single nucleotide polymorphisms (SNPs) while the remaining 10% represented insertions/deletions (Fig. S5D). This level of genetic variation between strains is consistent with the number of strain-specific SNPs and indels reported by other comparative genomic studies in *C. albicans* (38, 42, 63). Given the large number of genetic differences present between isolates, identification of variants associated with increased stability in the host GI tract would require extensive functional analyses which are beyond the scope of the current study.

SC5314, 529L, and CHN1 display similar morphologies in the GI tract. Since the ability of *C. albicans* to colonize the mammalian GI tract is associated closely with its propensity to filament (30, 31, 33, 34, 36, 64, 65), we directly assessed the morphology of CHN1, 529L, and SC5314 cells in the gut of C57BL/6J mice (RI). We utilized an antibiotic model of gut colonization to facilitate higher levels of fungal colonization than an antibiotic-free model, thereby enabling morphotypic analysis of fungal cells in GI tissue sections (see Fig. S6 for fecal and organ fungal burdens). Consistent with previous studies (33, 36), analysis of colon tissue sections colonized with SC5314 showed the presence of both yeast and filamentous forms (Fig. 4A). Colonization with 529L and CHN1 also revealed the presence of both morphological forms, both in the lumen and near the colon epithelium (Fig. 4A). Quantification of yeast and filamentous cells from different segments of the GI tract revealed that 529L exhibited slightly higher proportions of filamentous cells than SC5314 in the jejunum (18% more filamentous) but similar proportions of filamentous cells in the other GI segments (Fig. 4B). This result was unexpected given that 529L was defective for filamentation under most *in vitro* growth conditions (Fig. 3). In turn, CHN1 showed reduced filamentation in the duodenum relative to SC5314 (29% fewer filamentous cells) but the opposite trend in the colon (3% more filamentous cells [Fig. 4B]). These data demonstrate that, in general, clinical isolates 529L and CHN1 display a similar overall distribution of yeast and hyphal forms as SC5314 when colonizing the murine GI tract. The absence of consistent differences in cell morphology among the three isolates *in vivo* indicates that filamentation *per se* does not appear to drive differences in GI colonization.

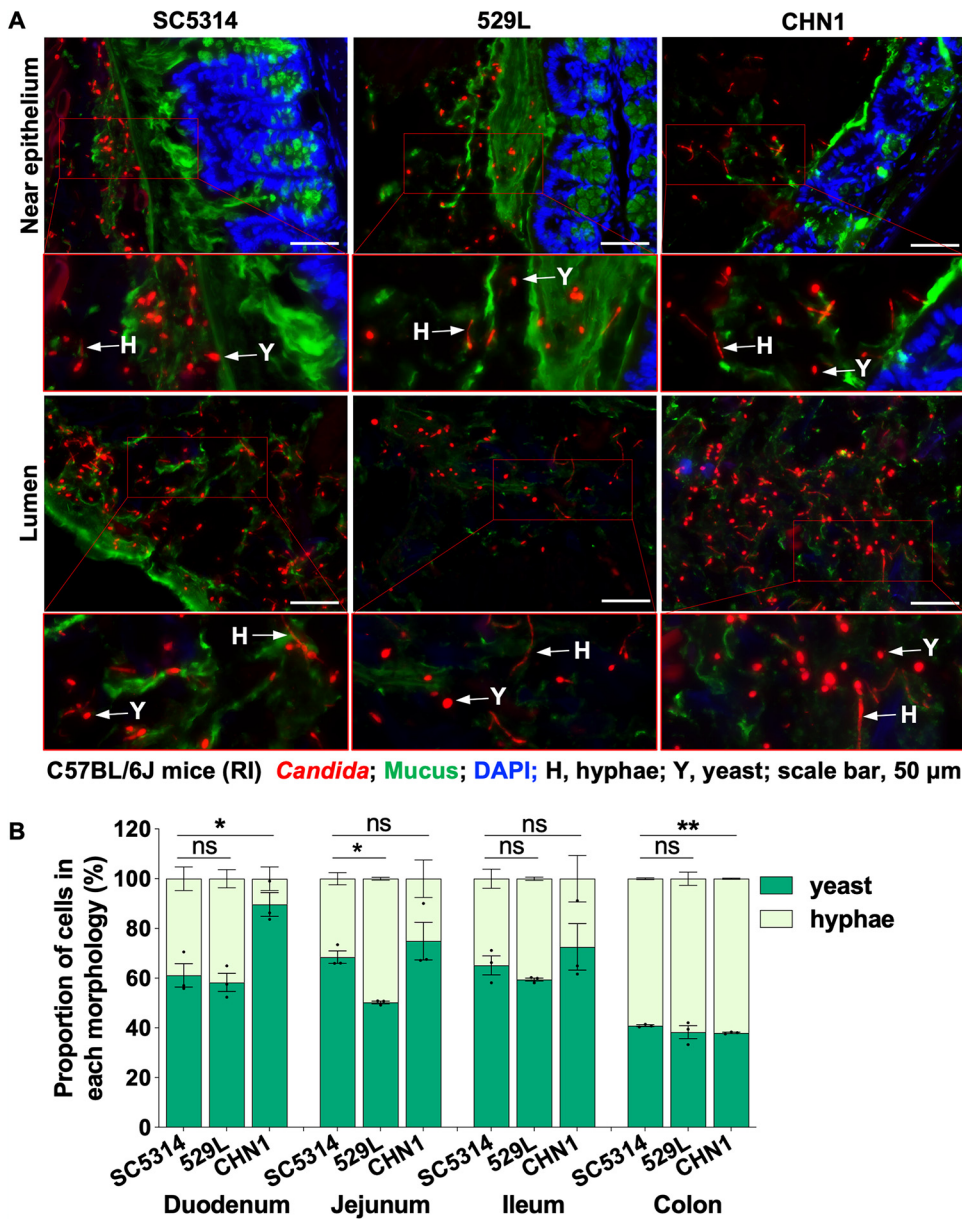


FIG 4 Morphology of *C. albicans* cells in the GI tract of C57BL/6J mice (RI) using an antibiotic model of colonization ($n = 3$ mice, single-housed). (A) FISH-stained *Candida* cells from colon sections. The colon tissues from mice were stained with a Cy3-coupled 28S rRNA fungal probe to stain both yeast and hyphal cells. Epithelium and mucus were stained with DAPI and UEA1/WGA1 coupled with fluorescein, respectively. Scale bar, 50 μm. Arrows indicate different *Candida* cell morphologies: H, hyphae; Y, yeast. (B) *Candida* cells in the different GI sections of C57BL/6J mice (RI) on antibiotics were stained with an anti-*Candida* antibody coupled with FITC. Histograms show the proportion (%) of yeast and hyphal cells in different GI organs (means ± SEM). Asterisks indicate statistical significance using unpaired parametric t tests: *, $P < 0.05$; **, $P < 0.01$; ns, not significant; $n = 50$ to 600 cells per section.

529L and CHN1 exhibit increased resistance to the antimicrobial peptide CRAMP relative to SC5314. The intestinal epithelium-derived antimicrobial peptide CRAMP was previously shown to inhibit *C. albicans* colonization in the murine GI tract (21). We hypothesized that *C. albicans* strains could be differentially sensitive to CRAMP, which may in turn affect their ability to colonize the GI niche. To test this, 529L, CHN1, and SC5314 were grown both aerobically and anaerobically at 37°C with different concentrations of the CRAMP peptide, and growth rates were monitored in real time (aerobic) or as endpoints (anaerobic). Under aerobic conditions, SC5314 growth was substantially inhibited by low concentrations of CRAMP (5 μM), and no growth was observed

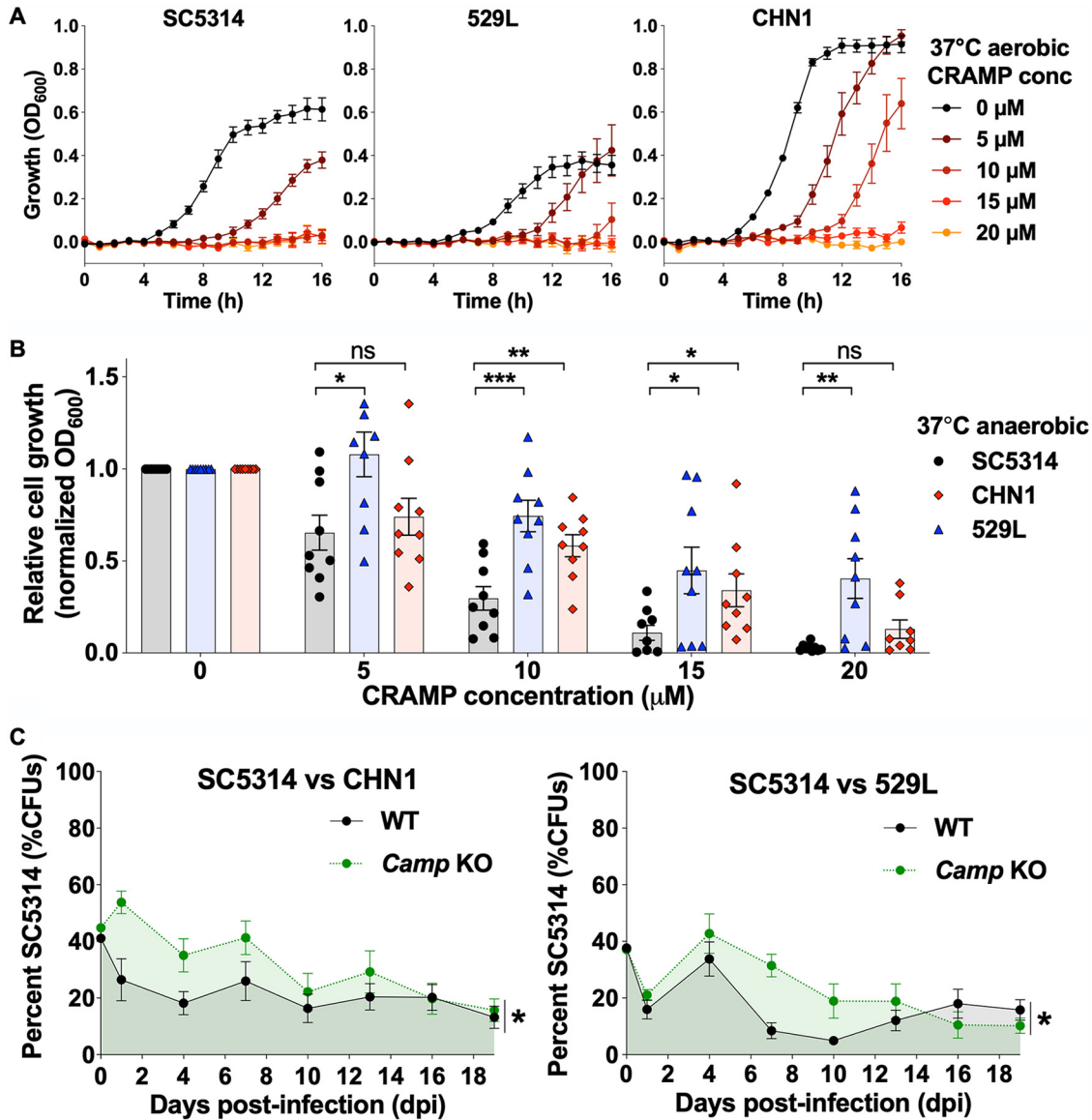


FIG 5 Effect of CRAMP on *C. albicans* growth and GI colonization. (A) *In vitro* susceptibility of *C. albicans* isolates SC5314, CHN1, and 529L to different CRAMP concentrations under aerobic growth at 37°C. Plots show growth levels (mean ± SEM) over 16 h from 3 biological replicates. (B) *In vitro* susceptibility of *C. albicans* isolates to different CRAMP concentrations at 37°C under anaerobic conditions. Histograms show mean relative fungal growth ± SEM values from 3 biological replicates. *, *P* < 0.05; **, *P* < 0.01; ***, *P* < 0.001, based on comparisons between SC5314 and CHN1 or 529L using unpaired parametric *t* tests. (C) Direct competitions between SC5314 and CHN1/529L in the GI tract of wild-type (WT) or *Camp* KO (C57BL/6J, TX) mice. Isolates were coinoculated in a 1:1 ratio, and the proportion (%) of SC5314 colonies was determined using nourseothricin selection upon recovery from fecal pellets. Plots show mean values ± SEM from 8 mice per group; *, *P* < 0.05, based on comparisons between WT and *Camp* KO curves using a linear mixed-effect model, a repeated-measures two-way ANOVA with Geisser-Greenhouse correction, and a log rank test.

with 10 μM CRAMP. In contrast, both 529L and CHN1 were more resistant to CRAMP and showed some ability to grow in the presence of a 10 μM concentration of this peptide (Fig. 5A).

Similar trends were obtained when strains were grown anaerobically; SC5314 growth was reduced by ~70% with 10 μM CRAMP whereas CHN1 and 529L showed an ~42% and an ~25% reduction in growth at this concentration (Fig. 5B). Differences between strains were also observed at higher concentrations, with 529L being the most resistant to CRAMP (Fig. 5B). These data establish that SC5314 is significantly more sensitive to CRAMP than CHN1 and 529L under both aerobic and anaerobic conditions *in vitro*. Inspection of *XOG1*, the *C. albicans* gene which encodes the β-(1,3)-exoglucanase targeted by LL-37/CRAMP (28, 66), did not

reveal genetic differences that could explain the differential sensitivity of the three isolates to this antimicrobial peptide (Fig. S5E).

To determine whether differences in CRAMP sensitivity could affect GI colonization, we performed direct competition experiments between SC5314 and CHN1 or 529L both in wild-type C57BL/6J mice and in *Camp* knockout (KO) mice that lack the gene encoding the CRAMP peptide. Mice were gavaged with an equal mix of strains, and the relative proportions of each strain were determined by analyzing nourseothricin-resistant/sensitive CFU in fecal pellets every 2 days. We found SC5314 showed a fitness defect relative to both CHN1 and 529L in mice regardless of whether they contained the *Camp* gene (Fig. 5C) (25, 67). However, SC5314 was present at a significantly higher proportion of the population in *Camp* KO mice than in control mice during the initial stages of colonization (first 10 to 14 days). Although a modest phenotype, this result implicates differences in GI colonization between CHN1/529L strains and SC5314 as being due, at least in part, to their differential susceptibility to the CRAMP antimicrobial peptide. This partial result is not unexpected given that multiple factors promote *C. albicans* colonization resistance in the gut, including other antimicrobial peptides (e.g., β -defensins [68]), metabolites (e.g., short-chain fatty acids [54]), and humoral factors (e.g., IgA [69]). As such, increased resistance to a single immune effector such as CRAMP would not be expected to completely explain the observed phenotypic differences.

DISCUSSION

C. albicans is a prevalent commensal of the human GI tract and yet is absent from the GI tract of most laboratory mouse strains. Moreover, colonization has typically required that adult mice are pretreated with antibiotics to enable stable colonization with SC5314, the standard *C. albicans* “laboratory” isolate. Here, we demonstrate that two alternative clinical isolates, CHN1 and 529L, allow for long-term colonization of the gut of adult mice even without antibiotic supplementation, whereas SC5314 is gradually lost from the GI tract under the same conditions. Colonization is particularly stable in C57BL/6J mice, which is the most widely used strain for biomedical research. We highlight that the increased stability of CHN1 and 529L over SC5314 was observed in multiple murine strains (C57BL/6J, BALB/c, and C3H/HeN) and in three separate animal facilities located in New York, Rhode Island, and Texas. This establishes that the increased colonization fitness of CHN1/529L relative to SC5314 is a general finding that is not unique to a single animal facility or mouse line and substantially expands the robustness of the current study. Our results therefore suggest that CHN1 and 529L will stably colonize the GI tract of mice in other animal facilities, establishing these strains as useful tools for researchers in the field. We also note that the fungal burdens observed using CHN1/529L in mouse lines were similar to those seen in patients with hematopoietic cell transplants (13).

A range of murine models have been used to study *C. albicans* colonization, yet most of these models use sustained antibiotic treatment with adult mice which results in variable colonization levels (12, 19, 20, 70–72). Neonatal models that utilize infant mice (~5 to 7 days of age) do not require antibiotic supplementation, which is attributed to an immature gut microbiota that lacks *Candida* colonization resistance (73, 74). Similarly, germ-free mice do not require antibiotics since they have no bacterial microbiota to inhibit *Candida* growth (21, 33, 75). Finally, diet modification using a low-fiber purified chow has also been shown to facilitate stable *Candida* gut colonization in mice even without antibiotics, presumably due to changes in the bacterial microbiome (18).

The current study highlights that intraspecies variation has a major impact on *C. albicans* commensalism among other attributes. Several intraspecies differences have previously been documented for *C. albicans* both *in vitro* and in systemic and oral infection models (37–39, 76). For example, while SC5314 is considered the standard lab isolate, this strain is one of the most virulent *C. albicans* strains in the murine systemic model (76) and shows a higher propensity to filament *in vitro* than other isolates (38). In most cases, the mechanisms by which intraspecies variation impacts fungal cell behavior have not been defined, although decreased genome heterozygosity and homozygosity of the mating type-like (*MTL*) locus have both been linked with reduced systemic virulence (37, 77, 78).

Interestingly, the niche from which clinical *C. albicans* strains are isolated generally does not correlate with their phenotypic properties, consistent with the idea that the same isolate can grow in multiple host tissues. Notable exceptions to this include a subclade of low-heterozygosity strains (clade 13, *Candida africana*) that show decreased virulence in animal models of infection and may be restricted to genital tract infections (42, 79) and hyperfilamentous *nrg1* mutants that have been repeatedly recovered from the lungs of cystic fibrosis patients (80). Loss of filamentation has also been observed in some clinical isolates and can enhance GI colonization of antibiotic-treated mice (34, 65). Previous findings have therefore established that natural variation can impact *C. albicans*-host interactions, and the current study adds to this concept by identifying strains that show differences in GI fitness in the absence of antibiotic treatment.

We note that 529L was obtained from a patient with oral candidiasis (47) while CHN1 was isolated from the human lung (48), indicating that these strains were not isolated from the intestinal tracts of their respective hosts. Laboratory experiments have shown that 529L can persistently colonize the murine oral cavity, unlike SC5314 (47), and this was linked to a decreased inflammatory response to 529L (39). Additional studies have documented instances in which strain variation impacted immune responses to *C. albicans* during a systemic infection and highlighted differences in cell wall architecture as possible causes for strain-specific phenotypes (81).

The CHN1 isolate has not been studied extensively and yet was previously shown to stably colonize the murine GI tract following pretreatment with cefoperazone, a broad-spectrum antibiotic (48, 82). SC5314 and CHN1 colonization behaviors were subsequently compared, and the two showed similar GI colonization properties in mice pretreated with this antibiotic (48). The ability of these two strains to alter the bacterial microbiota following antibiotic treatment was also evaluated, and both antagonized the regrowth of *Lactobacillus* (after cessation of antibiotic treatment) while promoting the growth of *Enterococcus*, indicating shared impacts on the bacterial microbiota (48). In the current study, we did not observe changes in the bacterial microbiota with colonization by SC5314, CHN1, or 529L. These differences in modulating the bacterial population are presumably due to differences in experimental design, with the current study showing that *C. albicans* colonization is not correlated with substantial changes to the composition of the bacterial microbiome.

Analysis of the *in vitro* phenotypes of SC5314, CHN1, and 529L revealed stark differences, with both CHN1 and 529L showing reduced metabolic and filamentation abilities relative to SC5314. 529L showed a particularly marked defect in growth and filamentation under a wide variety of conditions. However, all three strains showed similar propensities to filament in the GI niche, and 529L and SC5314 were previously shown to also exhibit similar filamentation phenotypes in the oral infection model (39). Our results indicate that *in vivo* filamentation characteristics can be very different from those observed *in vitro* and extend previous studies in which mutant *C. albicans* strains were shown to adopt different morphologies in the GI tract than those observed *in vitro* (36).

Sequencing of the 529L and CHN1 isolates did not reveal any obvious genetic alterations that might enable these strains to colonize mice better than SC5314. Thus, aneuploid configurations previously associated with increased fitness in the GI tract were not detected in these strains, although some homozygous tracts were shared by CHN1 and 529L that were absent in SC5314. However, the very large number of genetic differences among the three isolates makes identification of causal genetic links hard to establish without an extensive investigation of these differences.

It is likely that multiple mechanisms contribute to the observed strain differences in GI tract colonization, with the genetic and phenotypic differences described here likely to play important roles. We report that strain-specific differences in susceptibility to CRAMP, an intestine-derived antimicrobial peptide, could contribute to differences in colonization capacity, with SC5314 being more sensitive to this peptide than both 529L and CHN1. Interestingly, certain prominent gut commensal bacteria (including *Bacteroidetes*) are also more resistant to gut-derived antimicrobial peptides when

compared to gut pathobionts (e.g., *Escherichia coli*), which can promote the dominance of commensal gut microbiota over pathobionts in the gut (83). Thus, the multiple factors (genetic, phenotypic, and environmental) that modulate *Candida* susceptibility to antimicrobial peptides merit further investigation.

MATERIALS AND METHODS

Growth of *C. albicans* isolates. All *C. albicans* isolates used in this study are listed in Table S1 in the supplemental material. Unless otherwise specified, isolates were cultured overnight by picking 2 to 3 colonies and resuspending them in culture tubes containing 3 to 4 ml of liquid YPD (2% Bacto peptone, 1% yeast extract, 2% dextrose) at 30°C with shaking (200 to 250 rpm). Cell densities were measured using optical densities of culture dilutions (OD_{600}) in sterile water using a BioTek Epoch 2 plate reader.

Strain construction. To generate *SAT1*⁺ strains for GI competition assays, plasmid pDis3 was introduced into the *NEUT5L* neutral locus in the genome (53). The plasmid was linearized with NgoMIV and transformed into SC5314, CHN1, and 529L strains to generate *SAT1*⁺ transformants (Table S1), which were selected on YPD plus NAT (nourseothricin at 200 μ g/ml; Werner Bioagents). PCR with primers 3118 (CCCAGATGCGAAGTTAAGTGCGCAG) and 4926 (AAAAGGCCTGATAAGGAGAGATCCATTAAGAGCA) from reference 53 was used to check correct integration of the *SAT1* gene.

CRAMP *in vitro* assays. *C. albicans* isolates were grown overnight in synthetic complete medium (SC) at 30°C under aerobic conditions. Cells were inoculated in 3 ml of liquid SC at an OD_{600} of 0.25, grown at 30°C until reaching an OD_{600} of 1, harvested by centrifugation, and washed twice with 10 mM sodium phosphate buffer, pH 7.4 (NaPB). Cells were then resuspended in 3 ml of NaPB. Ten microliters of cell resuspension was added to 140 μ l YPD medium with or without the desired concentration of CRAMP (Anaspec; AS-61305) and incubated for 1 h at 37°C with shaking. Forty microliters of each culture was then added to an individual well of a 96-well plate containing 60 μ l YPD with the respective concentration of CRAMP. The plate was then incubated in a plate reader (BioTek Synergy HT) at 37°C with orbital shaking for 16 h. Growth was assessed by taking OD_{600} readings every hour. Aerobic experiments were performed with 3 biological experiments (with 3 technical replicates per biological experiment). For anaerobic growth in the presence of CRAMP, the 96-well plate was incubated at 37°C in an anaerobic chamber without shaking. Growth was evaluated by measuring the final biomass (OD_{600}) at the end of the 16 h incubation period. Anaerobic experiments were performed with 3 biological experiments (with 3 technical replicates per biological experiment).

Filamentation assays. For filamentation, *C. albicans* cells were grown overnight in YPD, washed in phosphate-buffered saline (PBS), and resuspended in PBS at a concentration of 10^5 cells/ml. One milliliter of cell suspension was added to 24-well plates containing different media, and plates were incubated for 4 h at 37°C with shaking. Images of approximately 500 to 1,000 cells were captured using a Zeiss Axio Observer microscope. Assays were performed with 3 biological replicates.

Phenotype microarray plate assays. *C. albicans* isolates were grown in YPD medium and then resuspended in sterile water to an OD_{600} of 0.2. The cell suspension was diluted 1:48 into inoculating fluid (IFY-0), and 100 μ l of the cell suspension was aliquoted into each well of Biolog PM1 and PM2 plates according to the manufacturer's instructions (Biolog Inc., Hayward, CA). The plate cultures were grown at 37°C for 24 h on a shaking platform at 200 rpm either aerobically or anaerobically (using Thermo Fisher AnaeroPack anaerobic gas generators in a sealed plastic bag). Following incubation, wells were scored for filamentation on a scale of 1 to 5 representing the proportion of filamentous cells in the population (1, 0 to 20%; 2, 20 to 40%; 3, 40 to 60%; 4, 60 to 80%; 5, 80 to 100%). PM experiments were performed with biological duplicates with growth (OD_{600}) and filamentation scores averaged across the two replicates. Correlation analyses between growth and filamentation were performed using a simple linear regression model in GraphPad Prism 9.

Gastrointestinal colonization and competition experiments. (i) Experiments in Rhode Island. For animal infections, 7- to 8-week-old female BALB/c (stock 028; Charles River Laboratories) or female C57BL/6J (stock 000664 from Jackson Laboratory, room MP14) mice were housed together with free access to food (standard rodent chow, LabDiet no. 5010, autoclaved) and water. *Candida* isolates were cultured overnight by picking 2 to 3 colonies and resuspending them in culture tubes containing 3 to 4 ml of liquid YPD at 30°C with shaking (200 to 250 rpm). Cell densities were determined by measuring optical densities of culture dilutions (OD_{600}) in sterile water using a BioTek Epoch 2 plate reader. Inocula were prepared by washing *Candida* cells and diluting them in sterile water to a concentration of 2×10^8 cells/ml. After 4 days of acclimation in the animal facility, mice were orally gavaged with 10^8 cells (0.5 ml volume) and fungal cells were isolated from fecal pellets every other day by plating for CFU. Pellets were homogenized in a PBS solution supplemented with an antibiotic mixture (500 μ g/ml penicillin, 500 μ g/ml ampicillin, 250 μ g/ml streptomycin, 225 μ g/ml kanamycin, 125 μ g/ml chloramphenicol, and 125 μ g/ml doxycycline). At the end of the experiment, mice were sacrificed and the number of fungal cells in each of the GI organs (stomach, small intestine, cecum, and colon) was determined by plating multiple dilutions of organ homogenates. For competition experiments, *C. albicans* cells were grown overnight in YPD at 30°C, washed with sterile water, and quantified. A quantity of 10^8 cells (containing a 1:1 ratio of each competing strain) was orally gavaged into the mouse GI tract. For each competition, one strain was nourseothricin sensitive (*SAT1*⁻) and one strain was nourseothricin resistant (*SAT1*⁺). Fecal pellets were collected every other day for 14 days, after which mice were euthanized and GI organs were collected for CFU determination. Abundance of each strain was quantified by plating the inoculum, organ, and fecal pellet homogenates onto YPD and YPD supplemented with nourseothricin (200 μ g/ml, Werner Bioagents).

(ii) Experiments in Texas. For GI colonization experiments with single-strain infection, 6- to 8-week-old C3H/HeN female mice were bought from Envigo (stock 040, C3H/HeNHsd). Mice were fed Teklad Global 16% protein rodent diet chow (Teklad 2916, irradiated). Mouse cages were changed once weekly.

Two to three *C. albicans* colonies were resuspended in 30 ml liquid YPD and grown for ~16 h at 30°C with shaking (200 rpm) under aerobic conditions. Cells were harvested, washed twice with PBS, and resuspended in PBS at a concentration of 1×10^9 CFU/ml. C3H/HeN female mice were gavaged with 200 μ l of cell suspension containing a total of 2×10^8 *Candida* cells. To determine fungal burdens, fecal pellets were collected every 7 days for 35 days, homogenized, and plated on YPD agar supplemented with antibiotics (30 μ g/ml of vancomycin and 30 μ g/ml of gentamicin).

For competition experiments, *C. albicans* isolates SC5314 (containing the *SAT1* gene, *SAT1*⁺), CHN1, and 529L were grown overnight in YPD at 30°C with shaking under aerobic conditions. Cells were harvested, washed twice with PBS, and resuspended in PBS at a concentration of 1×10^9 CFU/ml. Equal cell numbers of SC5314 (*SAT1*⁺) and CHN1 or 529L were mixed together. Six- to 8-week-old C57BL/6J (Jackson Laboratories, room RB12) or *Cramp* KO (Jackson Laboratories, stock 017799) female mice were gavaged with 200 μ l of cell suspension containing a total of 2×10^8 *Candida* cells. Equal strain ratios were confirmed by plating the initial inoculum. Fecal pellets were collected every 2 days for 19 days, homogenized, and plated on YPD agar supplemented with nourseothricin (200 μ g/ml) and antibiotics (30 μ g/ml of vancomycin and 30 μ g/ml of gentamicin).

(iii) Experiments in New York. C57BL/6J (stock 00664, Jackson Laboratory, room MP14) female mice were purchased in groups of 20 mice and redistributed between cages to normalize gut microbiome 1 week prior to use. Mice were fed Lab Diet 5053 (PicoLab rodent diet 20, irradiated). Mouse cages were changed once weekly. For GI colonization, *Candida* strains were streaked on SAB agar from glycerol stock and grown overnight at 37°C. Several colonies were collected into 2 ml YPD medium and grown for an additional 18 h at 30°C with shaking (250 rpm). Cells were then collected in water, and densities were measured using a hemocytometer. Mice were gavaged with 0.2 ml liquid culture containing a total of 10^7 cells per mouse. Fecal samples were collected prior to gavage and regularly over 48 days during colonization. Gut fungal burdens were determined by plating fecal pellet homogenates on SAB agar (BD Difco Sabouraud dextrose agar, BD 210930) plates supplemented with 10 μ g/ml of vancomycin (Hospira, NDC 0409-6510-01) and 100 μ g/ml of gentamicin (Gemini, 400108).

For GI competitions, *SAT1*⁻ and *SAT1*⁺ *Candida* strains were grown as described for GI colonization experiments. Mice were gavaged with 5×10^6 cells each of *SAT1*⁻ and *SAT1*⁺ strains (total of 10^7 cells per mouse). Fecal samples were collected regularly over 2 to 6 weeks and plated onto SAB and SAB with nourseothricin (100 μ g/ml, Gold Biotechnology, N-500-1) plates. Mice without detectable CFU are shown at the corresponding minimum detection level (50 to 100 CFU/g) across experiments and facilities. IACUC approval was obtained for animal experiments performed at all three facilities.

Analysis of *C. albicans* morphology in the mouse gut. *Candida* cells in the different GI sections were imaged by fluorescence *in situ* hybridization (FISH) as described in reference 36. In brief, C57BL/6J mice were treated with an antibiotic cocktail (penicillin, 1.5 mg/ml; streptomycin, 2 mg/ml; 2.5% glucose for taste) and fluconazole (0.5 mg/ml, Sigma-Aldrich) for 3 days, followed by antibiotic treatment for 1 day. At this point, the mice were colonized by adding *C. albicans* cells (2×10^5 cells/ml) to the drinking water containing antibiotics. The antibiotic-containing water was changed every 3 to 4 days. After 7 days of colonization, the mice were sacrificed, and the GI organs were harvested. One- to 2-cm pieces of different parts of the GI tract were fixed in methacarn (American Master Tech Scientific) overnight followed by two washes with 70% ethanol and subjected to paraffin block preparation. 10 μ m sections were first deparaffinized, and then the protocol from reference 36 was followed. *Candida* cells were stained with a Cy3-labeled panfungal 28S rRNA probe, epithelial cells were stained with 4',6-diamidino-2-phenylindole (DAPI) (Molecular Probes, Invitrogen), and the GI mucosal layer was stained with fluorescein-labeled WGA1 and UEA1 (Vector Laboratories). Tissue imaging was carried out using colon sections, and images were captured using a Zeiss Axio Observer microscope. Eight to 10 Z-stacks were merged to generate the final images.

To evaluate *Candida* morphology in the GI tract, 10 μ m tissue sections were first deparaffinized, blocked with $1 \times$ PBS plus 5% fetal bovine serum (FBS) for 30 min at room temperature, and then incubated with an anti-*Candida* antibody coupled to fluorescein isothiocyanate (FITC) (1:500 dilution; Biodesign International) overnight at 4°C. This was followed by 3 washes with PBS at room temperature and then staining of the epithelium with DAPI. Cell counting was carried out using an AxioVision Rel. 4.8 (Zeiss) fluorescence microscope. Two tissue sections from each mouse ($n = 3$ mice) were imaged, and 50 to 600 *Candida* cells per mouse were examined for morphology. The proportions of yeast and hyphal morphotypes were averaged for the two sections for each segment of the GI tract.

Whole-genome sequencing. To extract genomic DNA, isolates were grown overnight in YPD at 30°C and DNA was isolated from $\sim 10^9$ cells using a Qiagen genomic buffer set and a Qiagen Genomic-tip 100/G according to manufacturer's instructions. Libraries were prepared using the Nextera XT DNA library preparation kit protocol (Illumina) with an input of 2 ng/ μ l in 10 μ l. Each isolate was sequenced using Illumina HiSeq 2000, generating 101-bp paired reads. The nuclear genome sequences and General Feature Files (GFF) for *C. albicans* SC5314 reference genome (version A22) were downloaded from the *Candida* Genome Database (<http://www.candidagenome.org/>). Alignment, coverage, ploidy, heterozygosity, and variant calling were performed as previously described (84). Average coverage levels for SC5314, 529L, and CHN1 were $141 \times$, $466 \times$, and $245 \times$, respectively. Heterozygosity plots were constructed using methods from reference 42. Phylogenetic assignment was performed using RAxML (85) as described in reference 42 and using the isolates from the same study to classify the strains. Large homozygous tracts were confirmed by visual inspection in IGV (86). Mutations in *XOG1* were identified using GATK4 (87) and manually inspected in IGV. Genetic variants identified between SC5314 and 529L/CHN1 are included in Table S4 in the supplemental material.

16S sequencing. (i) Experiments in Rhode Island. DNA was extracted from samples using the ZymoBiomics Fecal/Soil DNA 96 kit from Zymo Research (D6011; Irvine, CA) per the manufacturer's instructions. Total DNA was eluted in nuclease-free water and quantified using the dsDNA-HS kit on a Qubit 3.0 fluorometer (Thermo Fisher Scientific, Waltham, MA). The 16S rRNA V4 hypervariable region was amplified from DNA using the barcoded 515F forward primer and the 806Rb reverse primers from the Earth Microbiome Project (88). Amplicons were generated using 5× Phusion high-fidelity DNA polymerase under the following cycling conditions: initial denaturation at 98°C for 30 s, followed by 25 cycles of 98°C for 10 s, 57°C for 30 s, and 72°C for 30 s, and then a final extension at 72°C for 5 min. Gel electrophoresis was used to confirm the amplicon size. The pooled amplicon library was sequenced at the Rhode Island Genomics and Sequencing Center at the University of Rhode Island (Kingston, RI) on the Illumina MiSeq platform with paired-end sequencing (2 × 250 bp), using the 600-cycle kit. Raw 16S rRNA reads were subjected to quality filtering, trimming, denoising, and merging using the Qiime2 pipeline (version 2018.11) (89). Taxonomic classification was done using the pretrained naive Bayes classifier and the q2-feature-classifier plugin trained on the SILVA 132 99% database. Beta diversity was calculated using the phyloseq package (version 1.30.0) (90) in R (version 3.6.2) and visualized using PCoA with a Bray-Curtis test. Raw sequence data were uploaded and made available on the NCBI Sequence Read Archive under BioProject number [PRJNA735873](https://www.ncbi.nlm.nih.gov/bioproject/PRJNA735873).

(ii) Experiments in New York. 16S DNA was extracted and purified from fecal samples collected on days 0 (before *Candida* gavage), 5, 12, and 48 after *Candida* gavage with a QIAamp kit (catalog no. 51306). The V4/V5 16S ribosomal DNA (rDNA) region was then PCR amplified using modified universal bacterial primers. PCR products were sent to IGO (Integrated Genomics Operation) for Illumina sequencing and library preparation. The sequences were then compared to the NCBI RefSeq RNA library, and raw reads were preprocessed using DADA2 implemented in R. DADA2 was used to perform quality filtering on resulting sequences, to infer exact amplicon sequence variants (ASVs) in resulting sequences, and to filter and remove chimeras (91). A minority of samples of insufficient quality were excluded from the analysis. Taxonomic assignment to species level was performed using an algorithm incorporating nucleotide BLAST (92), with NCBI RefSeq (93) as reference training set. The ASV tables, taxonomic assignment, and sample metadata were assembled using the phyloseq package construct (90). Construction of the sequence table and phyloseq object and all subsequent end-analyses were performed using R (version 3.4). Raw sequence data were uploaded on the NCBI Sequence Read Archive (SRA) under BioProject number [PRJNA734639](https://www.ncbi.nlm.nih.gov/bioproject/PRJNA734639) (see Table S2 for associated metadata). Beta diversity was visualized using PCoA with a Bray-Curtis test. Between-group differences were tested using a permutational multivariate ANOVA (PERMANOVA) (Adonis function via the Vegan package in RStudio 1.4) (94).

Data availability. Strains and plasmids are available upon request. Whole-genome sequencing data for SC5314, 529L, and CHN2 are available at NCBI SRA as BioProject [PRJNA730828](https://www.ncbi.nlm.nih.gov/bioproject/PRJNA730828). The raw sequence reads for SC5314 and 529L have been previously published on NCBI under BioProject [PRJNA193498](https://www.ncbi.nlm.nih.gov/bioproject/PRJNA193498) (38) for SC5314 and under accession numbers [SRX276261](https://www.ncbi.nlm.nih.gov/seq/submit/submit.cgi?accession=SRX276261) and [SRX276262](https://www.ncbi.nlm.nih.gov/seq/submit/submit.cgi?accession=SRX276262) for 529L (62). 16S raw reads are available on NCBI under BioProject numbers [PRJNA734639](https://www.ncbi.nlm.nih.gov/bioproject/PRJNA734639) and [PRJNA735873](https://www.ncbi.nlm.nih.gov/bioproject/PRJNA735873).

SUPPLEMENTAL MATERIAL

Supplemental material is available online only.

FIG S1, TIF file, 2.7 MB.

FIG S2, TIF file, 2.7 MB.

FIG S3, TIF file, 2.7 MB.

FIG S4, TIF file, 2.7 MB.

FIG S5, TIF file, 2.7 MB.

FIG S6, TIF file, 1.9 MB.

TABLE S1, XLSX file, 0.04 MB.

TABLE S2, XLSX file, 0.04 MB.

TABLE S3, XLSX file, 0.1 MB.

TABLE S4, XLSX file, 16.2 MB.

ACKNOWLEDGMENTS

We thank Mairi C. Noverr for the gift of the CHN1 strain.

This work was supported by National Institutes of Health (NIH) grants R01 AI093808 (T.M.H.), R01 AI139632 (T.M.H.), R21 AI105617 (T.M.H.), R21 AI156157 (T.M.H.), R01 AI123163 (A.Y.K.), K24 AI150992 (A.Y.K.), R01 AI141893 (R.J.B.), NIH R01 AI081704 (R.J.B.), NIH R21 AI144651 (R.J.B.), NIH R21 AI139592 (I.V.E.), NIGMS P20GM109035 (I.V.E.), P30 CA008748 (to MSKCC), R21AT010366 (P.B.), and NIDDK R01 DK125382 (P.B.). It was also supported by the Burroughs Wellcome Fund Investigator in the Pathogenesis of Infectious Diseases Award (T.M.H.), Ludwig Center for Cancer Immunotherapy (T.M.H.), Roberta I. and Normal L. Pollock Fund (A.Y.K.), Institut Pasteur G5 (I.V.E.), CIFAR Azrieli Global Scholar Award (I.V.E.), and an NSF Graduate Research Fellowship award 1644760 (S.P.). The funding agencies had no role in the design and preparation of the manuscript.

Designed research: L.D.M., A.A.M., N.T., B.Z., R.J.B., A.Y.K., T.M.H., I.V.E.; performed research: L.D.M., A.A.M., N.T., P.K., S.P., S.-H.L., B.Z., I.V.E.; analyzed data: L.D.M., A.A.M., N.T., P.K., S.P., S.-H.L., C.M., B.Z., Y.T., P.B., R.J.B., A.Y.K., T.M.H., I.V.E.; wrote the paper: L.D.M., A.A.M., N.T., R.J.B., A.Y.K., T.M.H., I.V.E.

A.Y.K. is a consultant for Prolacta Biosciences and receives research funding from Merck and Novartis. T.M.H. has participated in a scientific advisory board for Boehringer Ingelheim Pharmaceuticals, Inc.

REFERENCES

- Shao TY, Ang WXC, Jiang TT, Huang FS, Andersen H, Kinder JM, Pham G, Burg AR, Ruff B, Gonzalez T, Khurana Hershey GK, Haslam DB, Way SS. 2019. Commensal *Candida albicans* positively calibrates systemic Th17 immunological responses. *Cell Host Microbe* 25:404–417.e6. <https://doi.org/10.1016/j.chom.2019.02.004>.
- Jiang TT, Shao TY, Ang WXC, Kinder JM, Turner LH, Pham G, Whitt J, Alenghat T, Way SS. 2017. Commensal fungi recapitulate the protective benefits of intestinal bacteria. *Cell Host Microbe* 22:809–816.e4. <https://doi.org/10.1016/j.chom.2017.10.013>.
- Doron I, Leonardi I, Li XV, Fiers WD, Semon A, Bialt-DeCelle M, Migaud M, Gao IH, Lin WY, Kusakabe T, Puel A, Iliev ID. 2021. Human gut mycobiota tune immunity via CARD9-dependent induction of anti-fungal IgG antibodies. *Cell* 184:1017–1031.e14. <https://doi.org/10.1016/j.cell.2021.01.016>.
- Bacher P, Hohnstein T, Beerbaum E, Rocker M, Blango MG, Kaufmann S, Rohmel J, Eschenhagen P, Grehn C, Seidel K, Rickerts V, Lozza L, Stervbo U, Nienen M, Babel N, Milleck J, Assenmacher M, Cornely OA, Ziegler M, Wüplinghoff H, Heine G, Worm M, Siegmund B, Maul J, Creutz P, Tabeling C, Ruwwe-Glosenkamp C, Sander LE, Knosalla C, Brunke S, Hube B, Kniemeyer O, Brakhage AA, Schwarz C, Scheffold A. 2019. Human anti-fungal Th17 immunity and pathology rely on cross-reactivity against *Candida albicans*. *Cell* 176:1340–1355.e15. <https://doi.org/10.1016/j.cell.2019.01.041>.
- Limon JJ, Skalski JH, Underhill DM. 2017. Commensal fungi in health and disease. *Cell Host Microbe* 22:156–165. <https://doi.org/10.1016/j.chom.2017.07.002>.
- Gutierrez MW, Arrieta MC. 2021. The intestinal mycobiome as a determinant of host immune and metabolic health. *Curr Opin Microbiol* 62:8–13. <https://doi.org/10.1016/j.mib.2021.04.004>.
- van Tilburg Bernardes E, Pettersen VK, Gutierrez MW, Laforest-Lapointe I, Jendzjowsky NG, Cavin JB, Vicentini FA, Keenan CM, Ramay HR, Samara J, MacNaughton WK, Wilson RJA, Kelly MM, McCoy KD, Sharkey KA, Arrieta MC. 2020. Intestinal fungi are causally implicated in microbiome assembly and immune development in mice. *Nat Commun* 11:2577. <https://doi.org/10.1038/s41467-020-16431-1>.
- Nash AK, Auchtung TA, Wong MC, Smith DP, Gesell JR, Ross MC, Stewart CJ, Metcalf GA, Muzny DM, Gibbs RA, Ajami NJ, Petrosino JF. 2017. The gut mycobiome of the Human Microbiome Project healthy cohort. *Microbiome* 5:153. <https://doi.org/10.1186/s40168-017-0373-4>.
- Hoffmann C, Dollive S, Grunberg S, Chen J, Li H, Wu GD, Lewis JD, Bushman FD. 2013. Archaea and fungi of the human gut microbiome: correlations with diet and bacterial residents. *PLoS One* 8:e66019. <https://doi.org/10.1371/journal.pone.0066019>.
- Yan L, Yang C, Tang J. 2013. Disruption of the intestinal mucosal barrier in *Candida albicans* infections. *Microbiol Res* 168:389–395. <https://doi.org/10.1016/j.micres.2013.02.008>.
- Basmacıyan L, Bon F, Paradis T, Lapaquette P, Dalle F. 2019. *Candida albicans* interactions with the host: crossing the intestinal epithelial barrier. *Tissue Barriers* 7:1612661. <https://doi.org/10.1080/21688370.2019.1612661>.
- Koh AY, Kohler JR, Coggsall KT, Van Rooijen N, Pier GB. 2008. Mucosal damage and neutropenia are required for *Candida albicans* dissemination. *PLoS Pathog* 4:e35. <https://doi.org/10.1371/journal.ppat.0040035>.
- Zhai B, Ola M, Rolling T, Tosini NL, Joshowitz S, Littmann ER, Amoretti LA, Fontana E, Wright RJ, Miranda E, Veelken CA, Morjaria SM, Peled JU, van den Brink MRM, Babady NE, Butler G, Taur Y, Hohl TM. 2020. High-resolution mycobiota analysis reveals dynamic intestinal translocation preceding invasive candidiasis. *Nat Med* 26:59–64. <https://doi.org/10.1038/s41591-019-0709-7>.
- Iliev ID, Cadwell K. 2021. Effects of intestinal fungi and viruses on immune responses and inflammatory bowel diseases. *Gastroenterology* 160:1050–1066. <https://doi.org/10.1053/j.gastro.2020.06.100>.
- Wang T, Pan D, Zhou Z, You Y, Jiang C, Zhao X, Lin X. 2016. Dectin-3 deficiency promotes colitis development due to impaired antifungal innate immune responses in the gut. *PLoS Pathog* 12:e1005662. <https://doi.org/10.1371/journal.ppat.1005662>.
- Iliev ID, Funari VA, Taylor KD, Nguyen Q, Reyes CN, Strom SP, Brown J, Becker CA, Fleshner PR, Dubinsky M, Rotter JI, Wang HL, McGovern DP, Brown GD, Underhill DM. 2012. Interactions between commensal fungi and the C-type lectin receptor Dectin-1 influence colitis. *Science* 336:1314–1317. <https://doi.org/10.1126/science.1221789>.
- Yeung F, Chen YH, Lin JD, Leung JM, McCauley C, Devlin JC, Hansen C, Cronkite A, Stephens Z, Drake-Dunn C, Fulmer Y, Shopsis B, Ruggles KV, Round JL, Loke P, Graham AL, Cadwell K. 2020. Altered immunity of laboratory mice in the natural environment is associated with fungal colonization. *Cell Host Microbe* 27:809–822.e6. <https://doi.org/10.1016/j.chom.2020.02.015>.
- Yamaguchi N, Sonoyama K, Kikuchi H, Nagura T, Aritsuka T, Kawabata J. 2005. Gastric colonization of *Candida albicans* differs in mice fed commercial and purified diets. *J Nutr* 135:109–115. <https://doi.org/10.1093/jn/135.1.109>.
- Wiesner SM, Jechorek RP, Garni RM, Bendel CM, Wells CL. 2001. Gastrointestinal colonization by *Candida albicans* mutant strains in antibiotic-treated mice. *Clin Diagn Lab Immunol* 8:192–195. <https://doi.org/10.1128/CDLI.8.1.192-195.2001>.
- White SJ, Rosenbach A, Lephart P, Nguyen D, Benjamin A, Tzipori S, Whiteway M, Meccas J, Kumamoto CA. 2007. Self-regulation of *Candida albicans* population size during GI colonization. *PLoS Pathog* 3:e184. <https://doi.org/10.1371/journal.ppat.0030184>.
- Fan D, Coughlin LA, Neubauer MM, Kim J, Kim MS, Zhan X, Simms-Waldrup TR, Xie Y, Hooper LV, Koh AY. 2015. Activation of HIF-1alpha and LL-37 by commensal bacteria inhibits *Candida albicans* colonization. *Nat Med* 21:808–814. <https://doi.org/10.1038/nm.3871>.
- Matsuo K, Haku A, Bi B, Takahashi H, Kamada N, Yaguchi T, Saijo S, Yoneyama M, Goto Y. 2019. Fecal microbiota transplantation prevents *Candida albicans* from colonizing the gastrointestinal tract. *Microbiol Immunol* 63:155–163. <https://doi.org/10.1111/1348-0421.12680>.
- Kobayashi-Sakamoto M, Tamai R, Isogai E, Kiyoura Y. 2018. Gastrointestinal colonisation and systemic spread of *Candida albicans* in mice treated with antibiotics and prednisolone. *Microb Pathog* 117:191–199. <https://doi.org/10.1016/j.micpath.2018.02.043>.
- Shankar J, Solis NV, Mounaud S, Szpakowski S, Liu H, Losada L, Nierman WC, Filler SG. 2015. Using Bayesian modelling to investigate factors governing antibiotic-induced *Candida albicans* colonization of the GI tract. *Sci Rep* 5:8131. <https://doi.org/10.1038/srep08131>.
- Zhang M, Liang W, Gong W, Yoshimura T, Chen K, Wang JM. 2019. The critical role of the antimicrobial peptide LL-37/CRAMP in protection of colon microbiota balance, mucosal homeostasis, anti-inflammatory responses, and resistance to carcinogenesis. *Crit Rev Immunol* 39:83–92. <https://doi.org/10.1615/CritRevImmunol.2019030225>.
- Tsai PW, Cheng YL, Hsieh WP, Lan CY. 2014. Responses of *Candida albicans* to the human antimicrobial peptide LL-37. *J Microbiol* 52:581–589. <https://doi.org/10.1007/s12275-014-3630-2>.
- Tsai PW, Yang CY, Chang HT, Lan CY. 2011. Human antimicrobial peptide LL-37 inhibits adhesion of *Candida albicans* by interacting with yeast cell-wall carbohydrates. *PLoS One* 6:e17755. <https://doi.org/10.1371/journal.pone.0017755>.
- Tsai PW, Yang CY, Chang HT, Lan CY. 2011. Characterizing the role of cell-wall beta-1,3-exoglucanase Xog1p in *Candida albicans* adhesion by the human antimicrobial peptide LL-37. *PLoS One* 6:e21394. <https://doi.org/10.1371/journal.pone.0021394>.
- Lopez-Garcia B, Lee PH, Yamasaki K, Gallo RL. 2005. Anti-fungal activity of cathelicidins and their potential role in *Candida albicans* skin infection. *J Invest Dermatol* 125:108–115. <https://doi.org/10.1111/j.0022-202X.2005.23713.x>.
- Pierce JV, Dignard D, Whiteway M, Kumamoto CA. 2013. Normal adaptation of *Candida albicans* to the murine gastrointestinal tract requires

- Efg1p-dependent regulation of metabolic and host defense genes. *Eukaryot Cell* 12:37–49. <https://doi.org/10.1128/EC.00236-12>.
31. Pierce JV, Kumamoto CA. 2012. Variation in *Candida albicans* EFG1 expression enables host-dependent changes in colonizing fungal populations. *mBio* 3:e00117-12. <https://doi.org/10.1128/mBio.00117-12>.
 32. Pande K, Chen C, Noble SM. 2013. Passage through the mammalian gut triggers a phenotypic switch that promotes *Candida albicans* commensalism. *Nat Genet* 45:1088–1091. <https://doi.org/10.1038/ng.2710>.
 33. Bohm L, Torsin S, Tint SH, Eckstein MT, Ludwig T, Perez JC. 2017. The yeast form of the fungus *Candida albicans* promotes persistence in the gut of gnotobiotic mice. *PLoS Pathog* 13:e1006699. <https://doi.org/10.1371/journal.ppat.1006699>.
 34. Liang SH, Anderson MZ, Hirakawa MP, Wang JM, Frazer C, Alaalm LM, Thomson GJ, Ene IV, Bennett RJ. 2019. Hemizygoty enables a mutational transition governing virulence and commensalism. *Cell Host Microbe* 25:418–431.e6. <https://doi.org/10.1016/j.chom.2019.01.005>.
 35. Witchley JN, Basso P, Brimacombe CA, Abon NV, Noble SM. 2021. Recording of DNA-binding events reveals the importance of a repurposed *Candida albicans* regulatory network for gut commensalism. *Cell Host Microbe* 29:1002–1013.e9. <https://doi.org/10.1016/j.chom.2021.03.019>.
 36. Witchley JN, Penumetcha P, Abon NV, Woolford CA, Mitchell AP, Noble SM. 2019. *Candida albicans* morphogenesis programs control the balance between gut commensalism and invasive infection. *Cell Host Microbe* 25:432–443.e6. <https://doi.org/10.1016/j.chom.2019.02.008>.
 37. Wu W, Lockhart SR, Pujol C, Srikantha T, Soll DR. 2007. Heterozygosity of genes on the sex chromosome regulates *Candida albicans* virulence. *Mol Microbiol* 64:1587–1604. <https://doi.org/10.1111/j.1365-2958.2007.05759.x>.
 38. Hirakawa MP, Martinez DA, Sakthikumar S, Anderson MZ, Berlin A, Gujja S, Zeng Q, Zisson E, Wang JM, Greenberg JM, Berman J, Bennett RJ, Cuomo CA. 2015. Genetic and phenotypic intra-species variation in *Candida albicans*. *Genome Res* 25:413–425. <https://doi.org/10.1101/gr.174623.114>.
 39. Schonherr FA, Sparber F, Kirchner FR, Guiducci E, Trautwein-Weidner K, Gladiator A, Sertour N, Hetzel U, Le GTT, Pavelka N, d'Enfert C, Bougnoux ME, Corti CF, LeibundGut-Landmann S. 2017. The intraspecies diversity of *C. albicans* triggers qualitatively and temporally distinct host responses that determine the balance between commensalism and pathogenicity. *Mucosal Immunol* 10:1335–1350. <https://doi.org/10.1038/mi.2017.2>.
 40. Cavalieri D, Di Paola M, Rizzetto L, Tocci N, De Filippo C, Lionetti P, Ardizzoni A, Colombari B, Paulone S, Gut IG, Berna L, Gut M, Blanc J, Kapushesky M, Pericolini E, Blasi E, Peppoloni S. 2017. Genomic and phenotypic variation in morphogenetic networks of two *Candida albicans* isolates subtypes their different pathogenic potential. *Front Immunol* 8:1997. <https://doi.org/10.3389/fimmu.2017.01997>.
 41. Huang MY, Woolford CA, May G, McManus CJ, Mitchell AP. 2019. Circuit diversification in a biofilm regulatory network. *PLoS Pathog* 15:e1007787. <https://doi.org/10.1371/journal.ppat.1007787>.
 42. Ropars J, Maufrais C, Diogo D, Marcet-Houben M, Perin A, Sertour N, Mosca K, Permal E, Laval G, Bouchier C, Ma L, Schwartz K, Voelz K, May RC, Poulain J, Battail C, Wincker P, Borman AM, Chowdhary A, Fan S, Kim SH, Le Pape P, Romeo O, Shin JH, Gabaldon T, Sherlock G, Bougnoux M-E, d'Enfert C. 2018. Gene flow contributes to diversification of the major fungal pathogen *Candida albicans*. *Nat Commun* 9:2253. <https://doi.org/10.1038/s41467-018-04787-4>.
 43. Altamirano S, Jackson KM, Nielsen K. 2020. The interplay of phenotype and genotype in *Cryptococcus neoformans* disease. *Biosci Rep* 40:BSR20190337. <https://doi.org/10.1042/BSR20190337>.
 44. Kowalski CH, Beattie SR, Fuller KK, McGurk EA, Tang YW, Hohl TM, Obar JJ, Cramer RA, Jr. 2016. Heterogeneity among isolates reveals that fitness in low oxygen correlates with *Aspergillus fumigatus* virulence. *mBio* 7:e01515-16. <https://doi.org/10.1128/mBio.01515-16>.
 45. Demers EG, Biermann AR, Masonjones S, Crocker AW, Ashare A, Stajich JE, Hogan DA. 2018. Evolution of drug resistance in an antifungal-naive chronic *Candida lusitanae* infection. *Proc Natl Acad Sci U S A* 115:12040–12045. <https://doi.org/10.1073/pnas.1807698115>.
 46. Maestroni G, Semar R. 1968. Establishment and treatment of cutaneous *Candida albicans* infection in the rabbit. *Naturwissenschaften* 55:87–88. <https://doi.org/10.1007/BF00599501>.
 47. Rahman D, Mistry M, Thavaraj S, Challacombe SJ, Naglik JR. 2007. Murine model of concurrent oral and vaginal *Candida albicans* colonization to study epithelial host-pathogen interactions. *Microbes Infect* 9:615–622. <https://doi.org/10.1016/j.micinf.2007.01.012>.
 48. Mason KL, Erb Downward JR, Falkowski NR, Young VB, Kao JY, Huffnagle GB. 2012. Interplay between the gastric bacterial microbiota and *Candida albicans* during postantibiotic recolonization and gastritis. *Infect Immun* 80:150–158. <https://doi.org/10.1128/IAI.05162-11>.
 49. Naglik JR, Fidel PL, Jr, Odds FC. 2008. Animal models of mucosal *Candida* infection. *FEMS Microbiol Lett* 283:129–139. <https://doi.org/10.1111/j.1574-6968.2008.01160.x>.
 50. Solis NV, Filler SG. 2012. Mouse model of oropharyngeal candidiasis. *Nat Protoc* 7:637–642. <https://doi.org/10.1038/nprot.2012.011>.
 51. Fidel PL, Sobel JD. 1999. Murine models of *Candida* vaginal infections, p 741–748. In Zak O (ed), *Handbook of animal models of infection*. Academic Press, New York, NY.
 52. Koh AY. 2013. Murine models of *Candida* gastrointestinal colonization and dissemination. *Eukaryot Cell* 12:1416–1422. <https://doi.org/10.1128/EC.00196-13>.
 53. Gerami-Nejad M, Zacchi LF, McClellan M, Matter K, Berman J. 2013. Shuttle vectors for facile gap repair cloning and integration into a neutral locus in *Candida albicans*. *Microbiology (Reading)* 159:565–579. <https://doi.org/10.1099/mic.0.064097-0>.
 54. Guinan J, Wang S, Hazbun TR, Yadav H, Thangamani S. 2019. Antibiotic-induced decreases in the levels of microbial-derived short-chain fatty acids correlate with increased gastrointestinal colonization of *Candida albicans*. *Sci Rep* 9:8872. <https://doi.org/10.1038/s41598-019-45467-7>.
 55. Gunsalus KT, Tornberg-Belanger SN, Matthan NR, Lichtenstein AH, Kumamoto CA. 2016. Manipulation of host diet to reduce gastrointestinal colonization by the opportunistic pathogen *Candida albicans*. *mSphere* 1:e00020-15. <https://doi.org/10.1128/mSphere.00020-15>.
 56. Van Hauwenhuysse F, Fiori A, Van Dijck P. 2014. Ascorbic acid inhibition of *Candida albicans* Hsp90-mediated morphogenesis occurs via the transcriptional regulator Upc2. *Eukaryot Cell* 13:1278–1289. <https://doi.org/10.1128/EC.00096-14>.
 57. Nguyen LN, Lopes LC, Cordero RJ, Nosanchuk JD. 2011. Sodium butyrate inhibits pathogenic yeast growth and enhances the functions of macrophages. *J Antimicrob Chemother* 66:2573–2580. <https://doi.org/10.1093/jac/ckr358>.
 58. Liang W, Guan G, Dai Y, Cao C, Tao L, Du H, Nobile CJ, Zhong J, Huang G. 2016. Lactic acid bacteria differentially regulate filamentation in two hirable cell types of the human fungal pathogen *Candida albicans*. *Mol Microbiol* 102:506–519. <https://doi.org/10.1111/mmi.13475>.
 59. Murzyn A, Krasowska A, Stefanowicz P, Dziadkowiec D, Łukaszewicz M. 2010. Capric acid secreted by *S. boulardii* inhibits *C. albicans* filamentous growth, adhesion and biofilm formation. *PLoS One* 5:e12050. <https://doi.org/10.1371/journal.pone.0012050>.
 60. Forche A, Solis NV, Swidrigall M, Thomas R, Guyer A, Beach A, Cromie GA, Le GT, Lowell E, Pavelka N, Berman J, Dudley AM, Selmecki A, Filler SG. 2019. Selection of *Candida albicans* trisomy during oropharyngeal infection results in a commensal-like phenotype. *PLoS Genet* 15:e1008137. <https://doi.org/10.1371/journal.pgen.1008137>.
 61. Ene IV, Farrer RA, Hirakawa MP, Agwamba K, Cuomo CA, Bennett RJ. 2018. Global analysis of mutations driving microevolution of a heterozygous diploid fungal pathogen. *Proc Natl Acad Sci U S A* 115:E8688–E8697. <https://doi.org/10.1073/pnas.1806002115>.
 62. Cuomo CA, Fanning S, Gujja S, Zeng Q, Naglik JR, Filler SG, Mitchell AP. 2019. Genome sequence for *Candida albicans* clinical oral isolate 529L. *Microbiol Resour Announc* 8:e00554-19. <https://doi.org/10.1128/MRA.00554-19>.
 63. Wang JM, Bennett RJ, Anderson MZ. 2018. The genome of the human pathogen *Candida albicans* is shaped by mutation and cryptic sexual recombination. *mBio* 9:e01205-18. <https://doi.org/10.1128/mBio.01205-18>.
 64. Vautier S, Drummond RA, Chen K, Murray GI, Kadosh D, Brown AJ, Gow NA, MacCallum DM, Kolls JK, Brown GD. 2015. *Candida albicans* colonization and dissemination from the murine gastrointestinal tract: the influence of morphology and Th17 immunity. *Cell Microbiol* 17:445–450. <https://doi.org/10.1111/cmi.12388>.
 65. Tso GHW, Reales-Calderon JA, Tan ASM, Sem X, Le GTT, Tan TG, Lai GC, Srinivasan KG, Yurieva M, Liao W, Poidinger M, Zolezzi F, Rancati G, Pavelka N. 2018. Experimental evolution of a fungal pathogen into a gut symbiont. *Science* 362:589–595. <https://doi.org/10.1126/science.aat0537>.
 66. Chang HT, Tsai PW, Huang HH, Liu YS, Chien TS, Lan CY. 2012. LL37 and hBD-3 elevate the beta-1,3-exoglucanase activity of *Candida albicans* Xog1p, resulting in reduced fungal adhesion to plastic. *Biochem J* 441:963–970. <https://doi.org/10.1042/BJ20111454>.
 67. Yoshimura T, McLean MH, Dzutsev AK, Yao X, Chen K, Huang J, Gong W, Zhou J, Xiang Y, Badger JH, O'hUigin C, Thovarai V, Tessarollo L, Durum SK, Trinchieri G, Bian XW, Wang JM. 2018. The antimicrobial peptide CRAMP is essential for colon homeostasis by maintaining microbiota balance. *J Immunol* 200:2174–2185. <https://doi.org/10.4049/jimmunol.1602073>.

68. Schroeder BO, Wu Z, Nuding S, Groscurth S, Marcinowski M, Beisner J, Buchner J, Schaller M, Stange EF, Wehkamp J. 2011. Reduction of disulphide bonds unmasks potent antimicrobial activity of human beta-defensin 1. *Nature* 469:419–423. <https://doi.org/10.1038/nature09674>.
69. Bistoni F, Cenci E, Mencacci A, Schiaffella E, Mosci P, Puccetti P, Romani L. 1993. Mucosal and systemic T helper cell function after intragastric colonization of adult mice with *Candida albicans*. *J Infect Dis* 168:1449–1457. <https://doi.org/10.1093/infdis/168.6.1449>.
70. Mellado E, Cuenca-Estrella M, Regadera J, González M, Díaz-Guerra TM, Rodríguez-Tudela JL. 2000. Sustained gastrointestinal colonization and systemic dissemination by *Candida albicans*, *Candida tropicalis* and *Candida parapsilosis* in adult mice. *Diagn Microbiol Infect Dis* 38:21–28. [https://doi.org/10.1016/S0732-8893\(00\)00165-6](https://doi.org/10.1016/S0732-8893(00)00165-6).
71. de Repentigny L, Phaneuf M, Mathieu LG. 1992. Gastrointestinal colonization and systemic dissemination by *Candida albicans* and *Candida tropicalis* in intact and immunocompromised mice. *Infect Immun* 60:4907–4914. <https://doi.org/10.1128/iai.60.11.4907-4914.1992>.
72. Clemons KV, Gonzalez GM, Singh G, Imai J, Espiritu M, Parmar R, Stevens DA. 2006. Development of an orogastric mucosal model of candidiasis with dissemination to visceral organs. *Antimicrob Agents Chemother* 50:2650–2657. <https://doi.org/10.1128/AAC.00530-06>.
73. Pope LM, Cole GT, Guentzel MN, Berry LJ. 1979. Systemic and gastrointestinal candidiasis of infant mice after intragastric challenge. *Infect Immun* 25:702–707. <https://doi.org/10.1128/iai.25.2.702-707.1979>.
74. Domer JE. 1988. Intragastric colonization of infant mice with *Candida albicans* induces systemic immunity demonstrable upon challenge as adults. *J Infect Dis* 157:950–958. <https://doi.org/10.1093/infdis/157.5.950>.
75. Lopez-Medina E, Fan D, Coughlin LA, Ho EX, Lamont IL, Reimann C, Hooper LV, Koh AY. 2015. *Candida albicans* inhibits *Pseudomonas aeruginosa* virulence through suppression of pyochelin and pyoverdine biosynthesis. *PLoS Pathog* 11:e1005129. <https://doi.org/10.1371/journal.ppat.1005129>.
76. MacCallum DM, Castillo L, Nather K, Munro CA, Brown AJ, Gow NA, Odds FC. 2009. Property differences among the four major *Candida albicans* strain clades. *Eukaryot Cell* 8:373–387. <https://doi.org/10.1128/EC.00387-08>.
77. Hickman MA, Zeng G, Forche A, Hiraoka MP, Abbey D, Harrison BD, Wang YM, Su CH, Bennett RJ, Wang Y, Berman J. 2013. The ‘obligate diploid’ *Candida albicans* forms mating-competent haploids. *Nature* 494:55–59. <https://doi.org/10.1038/nature11865>.
78. Lockhart SR, Wu W, Radke JB, Zhao R, Soll DR. 2005. Increased virulence and competitive advantage of a/alpha over a/a or alpha/alpha offspring conserves the mating system of *Candida albicans*. *Genetics* 169:1883–1890. <https://doi.org/10.1534/genetics.104.038737>.
79. Borman AM, Szekeley A, Linton CJ, Palmer MD, Brown P, Johnson EM. 2013. Epidemiology, antifungal susceptibility, and pathogenicity of *Candida africana* isolates from the United Kingdom. *J Clin Microbiol* 51:967–972. <https://doi.org/10.1128/JCM.02816-12>.
80. Kim SH, Clark ST, Surendra A, Copeland JK, Wang PW, Ammar R, Collins C, Tullis DE, Nislow C, Hwang DM, Guttman DS, Cowen LE. 2015. Global analysis of the fungal microbiome in cystic fibrosis patients reveals loss of function of the transcriptional repressor Nrg1 as a mechanism of pathogen adaptation. *PLoS Pathog* 11:e1005308. <https://doi.org/10.1371/journal.ppat.1005308>.
81. Marakalala MJ, Vautier S, Potrykus J, Walker LA, Shepardson KM, Hopke A, Mora-Montes HM, Kerrigan A, Netea MG, Murray GI, MacCallum DM, Wheeler R, Munro CA, Gow NA, Cramer RA, Brown AJ, Brown GD. 2013. Differential adaptation of *Candida albicans* in vivo modulates immune recognition by dectin-1. *PLoS Pathog* 9:e1003315. <https://doi.org/10.1371/journal.ppat.1003315>.
82. Noverr MC, Noggle RM, Toews GB, Huffnagle GB. 2004. Role of antibiotics and fungal microbiota in driving pulmonary allergic responses. *Infect Immun* 72:4996–5003. <https://doi.org/10.1128/IAI.72.9.4996-5003.2004>.
83. Cullen TW, Schofield WB, Barry NA, Putnam EE, Rundell EA, Trent MS, Degnan PH, Booth CJ, Yu H, Goodman AL. 2015. Gut microbiota. Antimicrobial peptide resistance mediates resilience of prominent gut commensals during inflammation. *Science* 347:170–175. <https://doi.org/10.1126/science.1260580>.
84. Thomason GJ, Kakade P, Hiraoka MP, Ene IV, Bennett RJ. 2021. Adaptation to the dietary sugar D-tagatose via genome instability in polyploid *Candida albicans* cells. *G3 (Bethesda)* 11:jkab110. <https://doi.org/10.1093/g3journal/jkab110>.
85. Stamatakis A. 2014. RAxML version 8: a tool for phylogenetic analysis and post-analysis of large phylogenies. *Bioinformatics* 30:1312–1313. <https://doi.org/10.1093/bioinformatics/btu033>.
86. Thorvaldsdottir H, Robinson JT, Mesirov JP. 2013. Integrative Genomics Viewer (IGV): high-performance genomics data visualization and exploration. *Brief Bioinform* 14:178–192. <https://doi.org/10.1093/bib/bbs017>.
87. McKenna A, Hanna M, Banks E, Sivachenko A, Cibulskis K, Kernytzky A, Garimella K, Altshuler D, Gabriel S, Daly M, DePristo MA. 2010. The Genome Analysis Toolkit: a MapReduce framework for analyzing next-generation DNA sequencing data. *Genome Res* 20:1297–1303. <https://doi.org/10.1101/gr.107524.110>.
88. Thompson LR, Sanders JG, McDonald D, Amir A, Ladau J, Locey KJ, Prill RJ, Tripathi A, Gibbons SM, Ackermann G, Navas-Molina JA, Janssen S, Kopylova E, Vazquez-Baeza Y, Gonzalez A, Morton JT, Mirarab S, Zech Xu Z, Jiang L, Haroon MF, Kanbar J, Zhu Q, Jin Song S, Kosciorek T, Bokulich NA, Lefler J, Brislaw CJ, Humphrey G, Owens SM, Hampton-Marcell J, Berg-Lyons D, McKenzie V, Fierer N, Fuhrman JA, Clauset A, Stevens RL, Shade A, Pollard KS, Goodwin KD, Jansson JK, Gilbert JA, Knight R, Earth Microbiome Project Consortium. 2017. A communal catalogue reveals Earth’s multiscale microbial diversity. *Nature* 551:457–463. <https://doi.org/10.1038/nature24621>.
89. Hall M, Beiko RG. 2018. 16S rRNA gene analysis with QIIME2. *Methods Mol Biol* 1849:113–129. https://doi.org/10.1007/978-1-4939-8728-3_8.
90. McMurdie PJ, Holmes S. 2013. phyloseq: an R package for reproducible interactive analysis and graphics of microbiome census data. *PLoS One* 8:e61217. <https://doi.org/10.1371/journal.pone.0061217>.
91. Callahan BJ, McMurdie PJ, Rosen MJ, Han AW, Johnson AJ, Holmes SP. 2016. DADA2: high-resolution sample inference from Illumina amplicon data. *Nat Methods* 13:581–583. <https://doi.org/10.1038/nmeth.3869>.
92. Altschul SF, Gish W, Miller W, Myers EW, Lipman DJ. 1990. Basic local alignment search tool. *J Mol Biol* 215:403–410. [https://doi.org/10.1016/S0022-2836\(05\)80360-2](https://doi.org/10.1016/S0022-2836(05)80360-2).
93. Tatusova T, Ciufo S, Fedorov B, O’Neill K, Tolstoy I. 2014. RefSeq microbial genomes database: new representation and annotation strategy. *Nucleic Acids Res* 42:D553–D559. <https://doi.org/10.1093/nar/gkt1274>.
94. Tang ZZ, Chen G, Alekseyenko AV. 2016. PERMANOVA-S: association test for microbial community composition that accommodates confounders and multiple distances. *Bioinformatics* 32:2618–2625. <https://doi.org/10.1093/bioinformatics/btw311>.